AN ABSTRACT OF THE THESIS OF

Brooke Medley for the degree of Master of Science in Geography presented on March 18, 2008.
Title: A Method for Remotely Monitoring Glaciers with Regional Application to the Pacific Northwest

Abstract approved:

_____

Anne W. Nolin

An integrative method for monitoring glacier geometry change and mass balance is presented and applied to the Pacific Northwest, USA. Acting as a baseline for interpretation of future changes in glacier size and shape, we first derive a new inventory of regional glacier cover using remotely sensed data. To investigate current climate controls on glacier health, we next model glacier mass balance for select glaciers, incorporating glacier hypsometry results from our new remotely derived inventory. Model results are then used to interpret climate-glacier interactions through sensitivity analysis and the future impacts on glacier geometry. These steps when taken together create a method for remote monitoring of glacier health and dynamics that can be replicated globally.

Inventory results derived from the Advanced Spaceborne Thermal Emission and Reflection Radiometer imagery for the Pacific Northwest indicate that both the North Cascades National Park (99.0 ± 5.0 km^2) and the Cascade volcanoes of Washington and Oregon (96.0 ± 4.8 km^2) contain similar ice coverage while glaciers of the Olympic Mountains account for only 37.3 ± 1.9 km^2. Additionally, significant semi-annual variations in glacier coverage on the Cascade volcanoes highlight the need to consider recent mass balance variations when selecting satellite data for glacier inventorying.

Modeling results provided insight into climate-glacier interactions. Model results from the study glaciers show a recent strengthening of the relationship between summer balance and the El Niño/Southern Oscillation (ENSO) from the mid-1980s to the present. The correlation strengthening between ENSO and summer temperatures around 1985 is

manifested in our results through enhanced summer melt. However, the influence of the Pacific Decadal Oscillation (PDO) on balance fluctuations is more ambiguous, as the recent 1976/77 shift into a warm phase is weakly distinguishable at only one study glacier. Glacier sensitivity estimates for a 1° C rise in temperature range from -0.73 to -1.09 mw.e., decreasing with latitude; however, no discernible pattern of precipitation sensitivity exists. At South Cascade glacier, a 30% increase in winter precipitation could offset a 1° C rise in temperature. Glaciers further south require a >40% increase in winter precipitation to remain in balance. However, South Cascade is the only glacier of the four study glaciers that could not exist under a 2° C warming scenario as its accumulation area occupies very low elevations. We postulate that the sensitivity of South Cascade glacier does not change as rapidly as those of the remaining three glaciers as the glacier retreats, making it the most vulnerable to climate change.

A Method for Remotely Monitoring Glaciers with Regional Application to the Pacific Northwest

by
Brooke Medley

A THESIS

submitted to

Oregon State University

in partial fulfillment of
the requirements for the
degree of

Master of Science

Presented March 18, 2008
Commencement June 2008

Master of Science thesis of Brooke Medley presented on March 18, 2008

APPROVED:

_____

Major Professor, representing Geography

_____

Chair of the Department of Geosciences

_____

Dean of the Graduate School

I understand that my thesis will become part of the permanent collection of Oregon State University libraries. My signature below authorizes release of my thesis to any reader upon request.

_____

Brooke Medley, Author

ACKNOWLEDGEMENTS

I give many thanks to my advisor, Anne Nolin, for her support and guidance during my graduate tenure at Oregon State University. I also acknowledge members of my graduate committee, Zanna Chase, Peter Clark, and Julia Jones, for their insightful comments on the presented manuscripts. Finally, the model contribution of Wendell Tangborn is greatly appreciated in addition to his generous enthusiasm towards this project.

TABLE OF CONTENTS

TABLE OF CONTENTS (Continued)

Page

TABLE OF CONTENTS (Continued)

Page

LIST OF FIGURES

LIST OF FIGURES (Continued)

LIST OF TABLES

A Method for Remotely Monitoring Glaciers with Regional Application to the Pacific Northwest

Chapter 1 - Introduction

Glaciers constitute a vital link between climate and surface hydrology. Melt from these freshwater bodies contributes directly to sea level rise. Excluding the effect of thermal expansion, Meier *et al.* (2007) attribute all 20th century sea level rise to glacier melt, 60% of which originates from glaciers and ice caps outside of Greenland and Antarctica. Furthermore, they anticipate an additional 0.1 – 0.25 m rise in sea level from melting glaciers and ice caps during the 21st century. Total freshwater storage estimates from glaciers and ice caps in sea level equivalence range between 0.15 and 0.37 m (Lemke *et al.*, 2007). Compared to an estimated total sea level rise of 0.5 – 1.4 m asl by 2100 from Rahmstorf (2007), melt from glaciers and ice caps is a significant component of sea level rise over the next century. Glaciers are also capable of modulating regional freshwater supply as evidenced recently by Stahl and Moore (2006). They attribute recent negative trends in August streamflow for glacierized basins of British Columbia, Canada to regional ice loss. As a result, glacier loss can severely impact the success of regional agriculture and hydroelectric production. On a local scale, glaciers act as potential threats through catastrophic failure such as a debris flow. Chiarle *et al*. (2007) show debris flow frequency in the Italian Alps has risen during the past 25 years as significant glacier retreat has occurred. Therefore, fluctuations in ice cover are important considerations when investigating potential hydrologic impacts and risks associated with these important natural resources.

Glaciers of Oregon and Washington are of particular importance because they are rapidly losing mass, affecting the regional hydrologic cycle. According to recent estimates from Dyurgerov and Meier (2005), the 453.6 km^2 of glacier ice in these states constitutes 76% of total cover in the western U.S. highlighting the significance of the region. Additionally, they report some of the most rapid rates of ice loss have been observed in this region, indicating a changing role in surface hydrology. For example, Chennault (2006) attributes a decrease in late summer streamflow of >30% over the next

century due to ice loss alone in the North Cascades of Washington. Furthermore, recent glacier retreat might impact the magnitude of mass wasting event as a substantial volume of loose debris will be exposed. For example, during the 1980 Mount St. Helens eruption, voluminous debris flows or lahars washed down the slopes as the glaciers were obliterated. Driedger and Kennard (1986) estimate that ice volumes on Mount Rainier and Mount Hood are much larger than on Mount St. Helens prior to eruption. The proximity of Mt. Rainier and Mt. Hood to major metropolitan centers (Seattle, WA and Portland, OR respectively) makes them areas at risk. Because ice loss is expected to continue (Meier *et al.*, 2007), the environmental impacts of glacier retreat in Oregon and Washington are materializing.

To understand impact magnitude and potential in this region, we must first understand the main climate controls on glacier fluctuations. Therefore, a regional inventory of glaciers is necessary to act as a baseline for interpreting future changes in glacier size and shape. United States Geological Survey (USGS) topographic maps are a possible inventory source as they cover the entire region and can be acquired digitally for free. However, these maps are significantly outdated (20-50+ years) due to the short response time of alpine glaciers. Additionally, map compilation dates vary throughout the region making a single regional glacier snapshot unattainable. In response, we pose the question: *What is the current glacier distribution in Oregon and Washington?*

Because glacier geometry changes are both time-delayed and filtered responses to climate fluctuations, we cannot clearly determine the controlling mechanisms on these changes. Glacier mass balance observations on the other hand are neither time-delayed nor filtered and respond directly to climate and geometry fluctuations. Therefore, investigating regional mass balance measurements would allow for interpretations of climate controls on glacier health. When coupled with a current glacier inventory, we could then quantify future geometry and balance changes. Multiple glacier balance monitoring programs are in place in Washington providing crucial data for investigating climate-glacier interactions. However, the minimal temporal and spatial coverage of these datasets is limiting. Only Blue Glacier in the Olympic Mountains and South

Cascade Glacier in the North Cascades of Washington have sufficiently long (>30 years) records for analysis of climate controls on mass balance. Moreover, glacier sensitivity to specific climate variation cannot be determined, restricting our ability to make future predictions of glacier mass balance. For those reasons, we also ask: *How is glacier health in Washington and Oregon influenced by climate and what are reasonable expectations for changes in glacier size in the future?*

To answer the questions posed, we submit the following papers. The first paper, titled *Recent glacier variation in the Pacific Northwest incorporating a new remotely derived glacier inventory*, presents an updated glacier inventory for Oregon and part of Washington using satellite imagery from the 2000s. The second paper, titled *Model investigation of climate change impacts on glacier mass balance and geometry for four glaciers in the Pacific Northwest*, presents the results of a simple mass balance model for four glaciers, incorporating inventory results from the first paper. Model results are used to interpret climate-glacier interactions and their impact on glacier geometry. Our results provide an important link between local and global studies of glacier dynamics as well as improve estimates of the climate change impacts on glaciers in the region. Additionally, hydrologic forecasting models as well as debris flow hazard maps can be updated. Finally, these papers present a unique system for remote monitoring of glacier health and dynamics that can replicated globally.

Chapter 2 – First Manuscript

Recent glacier variation in the Pacific Northwest incorporating a new remotely derived glacier inventory

2.1 Abstract

A new inventory of glaciers derived from remotely sensed data is presented for the Pacific Northwest. Using USGS maps to form a baseline, glacier features were re-mapped using Advanced Spaceborne Thermal Emission and Reflection Radiometer (ASTER) imagery acquired from the 2000s. Additionally, short term variations of ice cover on individual strato-volcanoes are investigated. Glacier boundaries were mapped by taking the ratio of ASTER band 3 to band 4 and applying a threshold. Our ASTER inventory results of glacier coverage indicate that both the North Cascades National Park (99.0 ± 5.0 km^2) and the Cascade volcanoes of Washington and Oregon (96.0 ± 4.8 km^2) contain similar ice coverage, while glaciers of the Olympic Mountains account for only 37.3 ± 1.9 km^2. Significant annual variations in mapped glacier extent for the Cascade volcanoes highlight an important consideration when creating a glacier inventory from remotely sensed data. To accurately map permanent snow and ice features, images should be acquired following significant negative balance years, removing any seasonal snow features. Therefore, consideration of recent mass balance variations is crucial when selecting satellite data for glacier inventory derivation.

2.2 Introduction

Alpine glaciers and ice caps constitute only 3.2% of the global ice area; however, they are highly sensitive to climate fluctuations, providing a visible expression of climate change, and consequently monitoring their spatial coverage is critical as glaciers and ice caps will respond to climate fluctuations first (Ohmura, 2006). The retreat and thinning of these small glaciers account for about one-sixth of global sea level rise during the past century with a more recent increase in proportion to nearly one-half starting in 1990 (Dyurgerov and Meier, 1997). Ohmura (2004; 2006) estimates the ice stored by these glaciers is equivalent to a sea level rise of 15 cm, which is nearly identical to the *total* rise

experienced globally during the 20th century. Moreover, glaciers provide a significant regional freshwater resource (Barnett *et al.,* 2005). At a regional scale, changes in glacier extent modify the timing and magnitude of freshwater runoff, each of which play a critical role in the success of local agriculture and hydroelectric dams, as well as influence the potential for natural catastrophes (e.g., glacial outburst floods, landslides, debris flows). For these reasons, regional glacier monitoring is justified.

Our study provides a recent glacier inventory for part of the Pacific Northwest, USA, including the Cascade and Olympic mountain ranges. Regional fluctuations in glacier area are obtained through the use of aerial photography (e.g., Granshaw and Fountain, 2006) and satellite imagery (e.g., Paul *et al.*, 2004). Ideally, glacier mass balance would be monitored as it is a direct and instantaneous indicator of climate change, but measurements are too laborious and expensive for a regional mass balance observation program. Although glacier area change is a time-delayed climate signal as alpine glaciers respond to climate fluctuations on the order of years to decades (Barry, 2006), changes can be monitored over large areas and are particularly informative for regional scale studies.

This study uses the unique spectral characteristics of snow/ice to map glacier cover using recent ASTER imagery. Our ASTER results are juxtaposed with a USGS baseline inventory to analyze the long-term change in cover. Finally, we relate short-term (annual) changes in mass balance and area changes to aid in our interpretation of the ASTER inventory results.

2.3 Regional Setting and Significance

Glaciers of the Pacific Northwest are classified into three sub-regions based on their distinct glacier setting (Figure 2.1). On the Cascade volcanoes, glaciers and perennial snowfields are restricted to the highest of peaks. Large volumes of snow and ice are concentrated on individual volcanoes, creating the largest glaciers (> 10 km^3) in the entire Pacific Northwest (Driedger and Kennard, 1986). Ranging in elevation from approximately 1500 m to over 4000 m, glaciers on the high peaks (i.e. Three Sisters,

Jefferson, Hood, Adams, and Rainier) typically have distinct boundaries at lower elevations and often coalesce closer to the summit. Altogether these peaks once sustained nearly 150 km^2 of ice (Meier, 1961a; Driedger and Kennard, 1986), providing an important natural resource as well as a potential hazard.

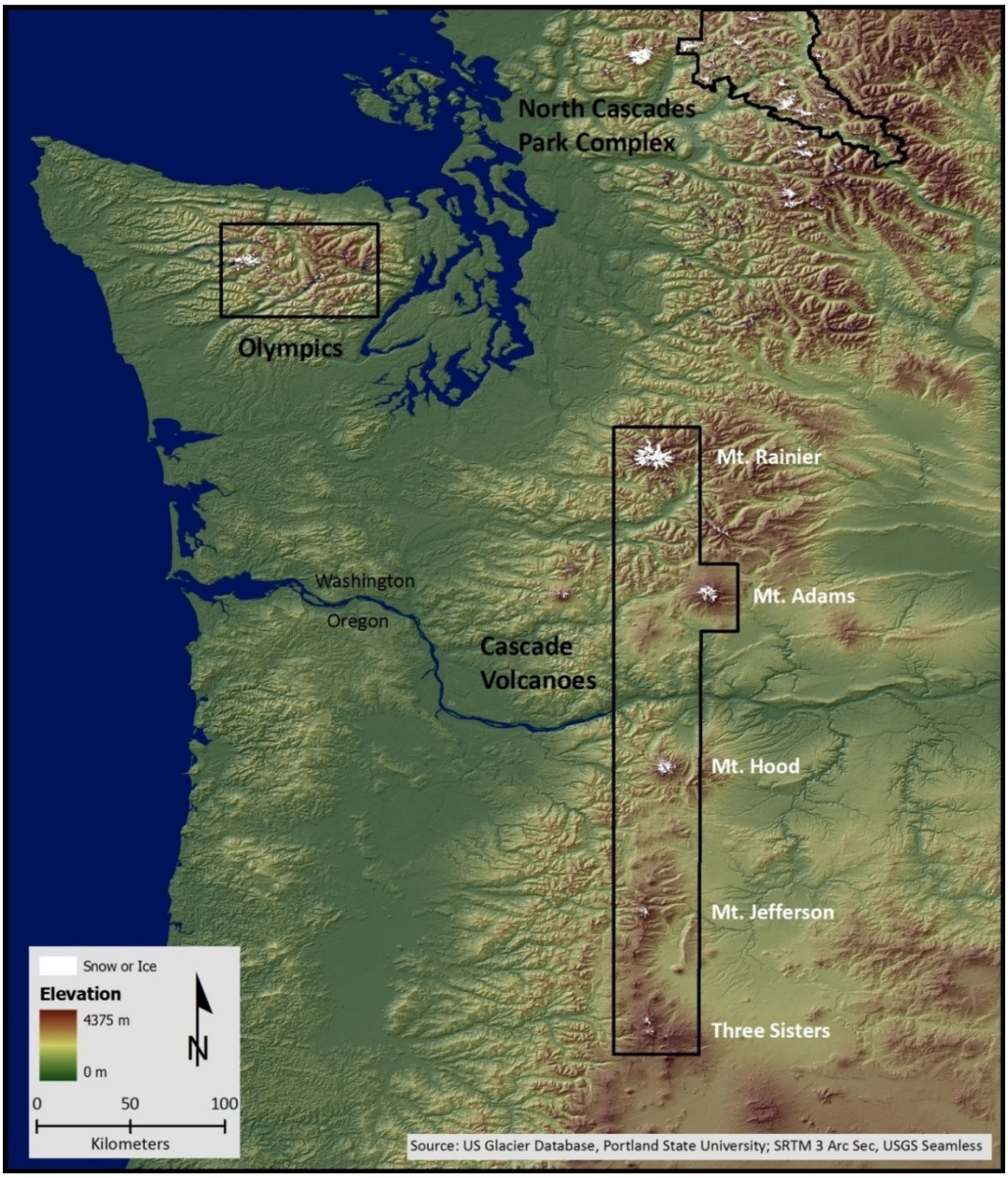

Figure 2.1: Location of the three sub-regions (NOCA, Olympics, Cascade Volcanoes) outlined in black. Glacier distribution from 1:100k USGS topographic maps is overlaid on regional topography.

In the North Cascades of Washington, snow and ice become a more prominent characteristic of the landscape, blanketing high peaks and ridgelines. Glaciers in this sub-region are dispersed and exist at elevations between 1085 m and 2700 m. Even though the largest glacier is < 7 km^2, nearly 800 glaciers inhabit 267 km^2 in the state of Washington (Post *et al.*, 1971). This research investigates only glacier features of the North Cascades Park Complex (NOCA) outlined in Figure 2.1.

The glaciers of the Olympic Mountains are distinct, occupying the lowest of elevations from 1000 m to 2400 m. Their proximity to the Pacific Ocean (~ 50 km) produces the wet climate necessary to sustain ice at such relatively low elevations. According to a previous glacier inventory by Spicer (1986), total ice cover is 46 km^2 consisting of > 250 glaciers.

Although the physiographies of these sub-regions are unique, they provide a common resource: meltwater. In the NOCA, two of the major basins fed by glacier melt have five hydroelectric dams (Granshaw and Fountain, 2006). Results presented by Chennault (2004) indicate that glacial meltwater in the most heavily glaciated basin of the North Cascades makes up between ~0 to >50% of late summer streamflow between 1998 and 2002. Furthermore, ice melt supplies water to the river systems throughout the summer when precipitation is minimal in the Pacific Northwest. For example, during the driest months of summer, glacier meltwater constitutes nearly three-fourths of the flows into the irrigation districts on the upper Middle Fork Hood River (Nolin and Phillippe, personal communication), an agricultural district containing some of the highest value crops in Oregon. Furthermore, unlike the seasonal snowpack, glaciers are capable of minimizing interannual extremes. During a year with minimal snowpack, ice persists through the summer as the only meltwater source, minimizing the severity of a drought. Glaciers additionally store excess snow for future use during a year with a healthy snowpack. Chennault (2004) determined the largest proportions of glacier meltwater in late summer streamflow came during warm and dry years and the smallest proportions came during wet and cool years. Any loss in glacier area could lead to an increase in runoff variability since valuable freshwater storage would be lost.

Storing water as snow or ice is also a risk, as catastrophic melting can result in a massive disaster. Substantial warm rain in contact with snow and ice can cause rapid melting, leading to powerful debris flows. A more extreme variation can occur on the glaciated volcanoes during an eruption. During the 1980 Mount St. Helens eruption, voluminous debris flows or lahars washed down the slopes as the glaciers were obliterated. Driedger and Kennard (1986) estimate that ice volumes on Mount Rainier and Mount Hood are much larger than on Mount St. Helens prior to eruption. The proximity of Rainier and Hood to major metropolitan centers (Seattle, WA and Portland, OR respectively) identifies them as areas of high risk. Monitoring changes in glacier area allows for more accurate assessments of ice volume, an extremely important variable when creating hazards maps and evacuation plans for volcanic eruptions.

Furthermore, the high peaks of the Pacific Northwest are famous for their dramatic, ice-draped slopes, making them popular tourist destinations. Approximately 2.75 million people visited Olympic National Park for recreational purposes in 2006, a number on par with other parks in the American West such as Grand Teton, Yellowstone, and Rocky Mountain and overshadows the 1.9 million that visited Glacier National Park (NPS, 2007). Mount Rainier National Park alone drew in 1.1 million visitors. Additionally, Mount Hood ranks as the second most climbed glaciated peak in the world. However, maps of these glaciers are outdated, a potential hazard for hikers and visitors. Updating the glacier inventory in the Pacific Northwest will minimize the potential impact of these hazards.

2.4 Previous Work

2.4.1 Glacier Inventories

Studies of glacier area changes in these sub-regions are rare, and instead glaciers have been either monitored individually (e.g., Heliker *et al.*, 1984; Krimmel, 1989; Spicer, 1989) or on a single peak (e.g., Howat *et al.*, 2006; Lillquist and Walker, 2006). The first extensive inventory of ice cover was completed by Meier (1961a) using maps and aerial photographs produced by the United States Forest Service (USFS) and Geological Survey

(USGS). Over 1,000 glaciers covering 513 km^2 were measured throughout the entire American West, with an estimated 77% residing in the state of Washington. Selected results are presented in Table 2.1. In 1971, a more detailed survey of glaciers in the North Cascades was published by Post and others. Over 750 glaciers were mapped, accounting for 267 km^2; the NOCA consists of 116 km^2 alone. Granshaw and Fountain (2006) further determined the Park has experienced a loss of about 8 km^2 in the 40 year period since the 1958 Post *et al.* (1971) inventory. Work completed by Driedger and Kennard (1986) presented an updated survey of glaciers on three Cascade volcanoes (Table 2.1). Mount Rainier is the most glaciated with nearly seven times the ice cover of Mount Hood, the second most glaciated of the three. Spicer (1986) completed an inventory of glaciers in the Olympic Mountains finding 266 glaciers covering 45.9 km^2. Aside from the NOCA, recent surveys of regional glacier extent do not exist. This study provides new estimates of glacier cover for all three sub-regions – the NOCA, Olympics, and Cascade Volcanoes – using satellite remote sensing.

Table 2.1: Glacier area from multiple inventories

Location	Meier (1961a)	Update[2]
Washington		
North Cascades Park Complex	115.6[1]	109.1[3]
Olympics	33.0	45.9[4]
Mount Rainier	87.8	92.1
Mount Adams	16.1*	--
Oregon		
Mount Hood	9.9	13.5
Mount Jefferson	3.2	--
Three Sisters	7.6	8.3

[1] Post *et al.* (1971)
[2] Driedger and Kennard (1986) unless noted
[3] Granshaw and Fountain (2006)
[4] Spicer (1986)
* Estimated value

2.4.2 Snow/Ice Remote Sensing

Snow and ice constitute two of the visibly brightest materials on Earth. However, in the near-infrared (NIR) part of the electromagnetic spectrum, snow and ice are extremely dark, absorbing more incident radiation. Such contrast is unique to snow and ice, a characteristic that facilitates the mapping of glacier ice from space. Furthermore, Hall *et* al. (2002) determined that snow-cover mapping derived from visible and NIR data is more accurate than passive-microwave data. However, caution must be taken when using satellite imagery to ensure that what is indentified remotely actually represents the material on the surface of the Earth. For instance, no simple method for distinguishing between snow and ice exists; therefore, perennial snow fields might be mapped as glacier ice. We attempt to minimize this issue by mapping features for multiple years and selecting the coverage with the smallest area which we assume as representative of the resistant ice bodies only.

The amount of radiation reflected by snow and ice is dependent on many variables such as debris cover, age, and solar and sensor geometry. Near glacier margins, oversteepened moraines can deposit loose rock onto the ice surface (Benn and Evans, 1998). This debris cover acts as a shield covering the snow and ice underneath it and is difficult to spectrally differentiate from the rocky moraines nearby. Also, the surface albedo of snow and ice is significantly diminished with age. Solar and sensor positions as well as the surface slope and aspect affect surface reflectance as well.

Nonetheless, glacier mapping using satellite imagery is an extremely accurate and straightforward process. Paul *et al.* (2002) created an updated Swiss glacier inventory using multispectral satellite imagery. The authors analyzed multiple methods for glacier mapping to assess their accuracy. Although there are many different approaches to delineating glacier outlines (e.g., manual digitization, band ratios, supervised and unsupervised classifications), both Paul (2002a;b) and Albert (2002) determined that thresholding the ratio of Landsat Thematic Mapper band 4 to band 5 resulted in the most accurate and cost-effective product, finding the method 97% and 92% accurate

respectively for debris-free ice. In this study we use the band ratio method using equivalent ASTER bands.

2.5 Methodology

To accurately map glaciers in the Pacific Northwest, a baseline inventory is needed as a guide to further mapping and a basis for change detection. USGS topographic maps were acquired and using a Geographic Information System (GIS), glacier outlines were mapped to create a baseline. A second inventory was created using ASTER data, mapping only the glaciers outlined in the initial baseline inventory.

2.5.1 Creating a baseline

To reconstruct glacier extent, digital USGS Topographic Quadrangle maps were acquired for the Olympics and Cascade Volcanoes. Digital outlines for both 1958 and 1998 glacier coverages in the NOCA are available from Granshaw (2002). The baseline year is not constant throughout the region as the USGS topographic maps were created from different photographic surveys. Survey dates vary from 1959 to 1987 and are presented in Table 2.2. We refer to this baseline at the USGS inventory, which incorporates multiple coverage years.

Table 2.2: Representative years used in inventories

Location	USGS	ASTER
North Cascades	1958	2006[1]
Olympics	1987	2004[2]
Cascade Volcanoes		
Rainier	1970	2005
Adams	1969	2005
Hood	1956	2003
Jefferson	1949	2006
Three Sisters	1958	2003

[1] Contains some results from 2005
[2] Contains some results from 2002

2.5.2 Creating a current inventory

Acquiring an image from the end of the water year is required, eliminating the misclassification of seasonal snow patches as glacier ice. Most scenes used in this study were collected from September or October with some from late August. Figure 2.2 is a false color ASTER image of South Cascade glacier from September 27, 2003. The authors attempted to obtain imagery for all glaciers each year between 2000 and 2006. Complications with cloud cover and lack of sensor coverage allowed for a single inventory for the NOCA and Olympics. We were able to map the glaciers of the Cascade Volcanoes multiple years (2-5) allowing us to investigate short term fluctuations.

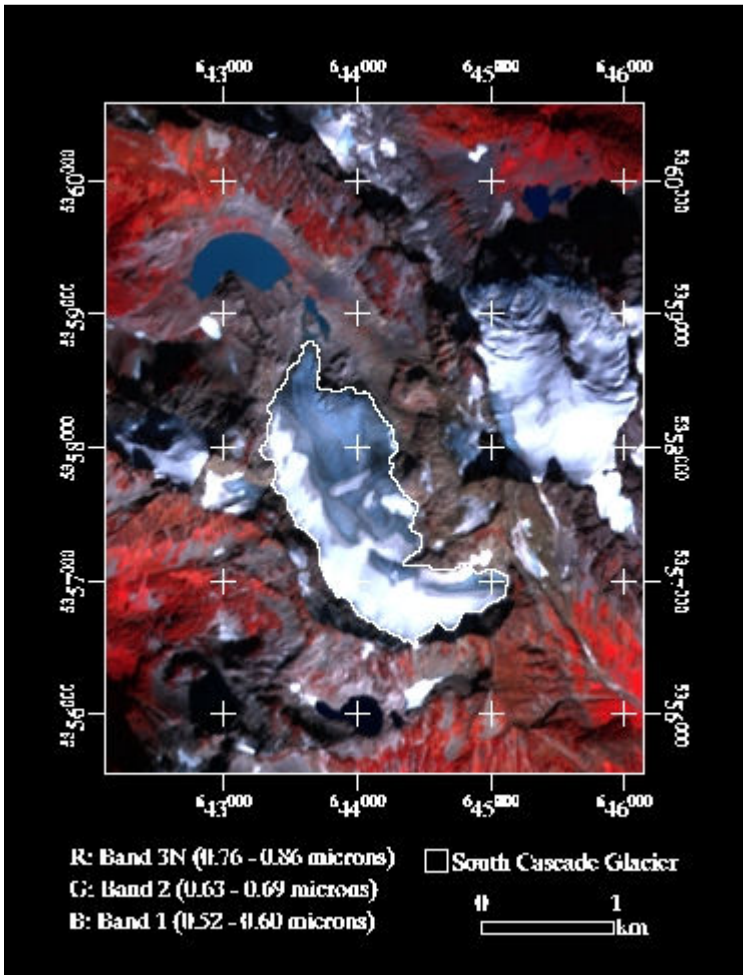

Figure 2.2: ASTER derived 2003 South Cascade glacier boundary. The glacier is overlaid on an RGB composite image using ASTER visible bands.

This study uses the orthorectified ASTER product. Each scene covers approximately 60 km x 60 km, containing data at 15 m, 30 m, and 90 m spatial resolutions depending on spectral coverage. Here, we use ASTER bands 3N (0.76 - 0.86 μm) and 4 (1.60 - 1.70 μm) with respective spatial resolutions of 15 m and 30 m. Atmospheric correction using the method of dark pixel subtraction (Chavez, 1975) was performed on each scene in order to minimize any atmospheric effects.

As previous studies have relied on the ratio of radiance in visible and NIR channels to discriminate between snow/ice and other land surface materials (Dozier, 1989; Hall *et al*, 2002), we use a similar approach but have modified it to suit ASTER imagery. Following preprocessing, a pilot study on South Cascade Glacier was undertaken to determine the threshold value used to discriminate snow and ice from other materials. The ASTER Band 3/Band 4 ratio was calculated for the area encompassing South Cascade Glacier in 2003and 2005 (see Figure 2.3 for an example). Using area calculations from Bidlake and others (2005; 2007), multiple ratio thresholds were tested but only one was selected based on its ability to most accurately reproduce actual area measurements. A threshold of 2.5 produced area estimates of 1.75 km^2 in 2003 and 1.69 km^2 in 2005 with an average accuracy of 95%. It is appropriate to note that South Cascade Glacier is essentially free of any debris cover, limiting method accuracy to clean ice. Furthermore, we define glaciers and perennial snowfields as *permanent* landscape features; however, we understand that on longer timescales, these features might not be defined as such.

Glaciers elsewhere are now mapped automatically by invoking an ice threshold of 2.5 for each ASTER Band 3/Band 4 ratio image. The results are filtered to include only those bodies mapped in the baseline to make direct comparisons between the two inventories. For the Cascade Volcanoes where features were mapped multiple years, the smallest area estimate was selected for the ASTER inventory in order to minimize the inclusion of *non-permanent* snow and ice features. Years selected for the inventory are presented in Table 2.2.

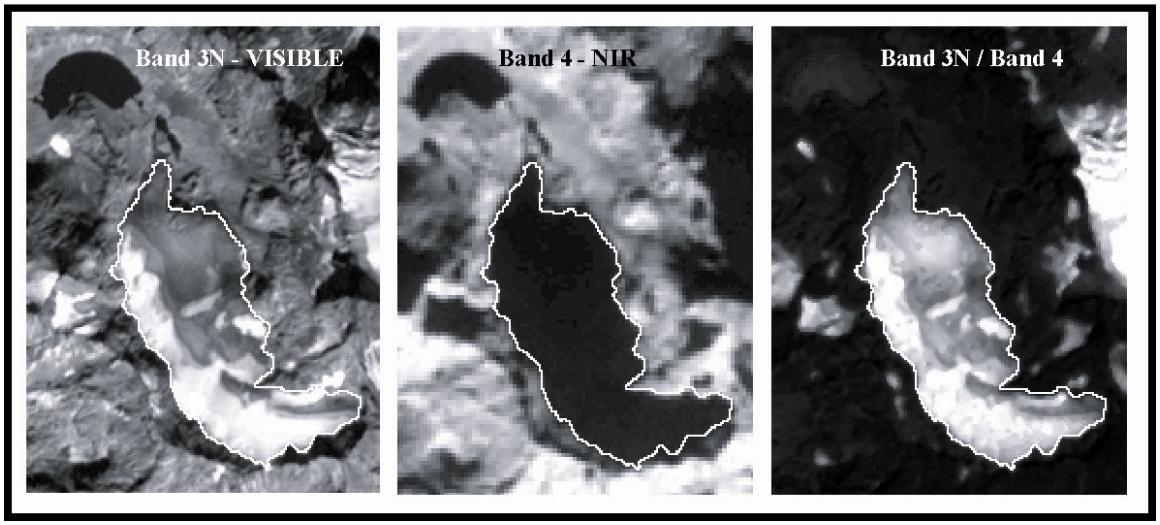

Figure 2.3: Digital number images for ASTER bands 3N and 4 and their ratio at South Cascade glacier. Imagery was captured September 27, 2003.

2.5.3 Estimating Error

Error estimation differed between the USGS and ASTER inventories. Using the same method as Granshaw and Fountain (2006), the USGS inventory error was calculated based on positional accuracy (12.2 m) and digitizing error (2.4 m). The uncertainty in the USGS area estimates was determined as the area of a buffer around each glacier of twice the root mean square of the aforementioned errors (6.2 m). ASTER mapping accuracy was calculated through comparison with actual glacier area measurements at South Cascade Glacier. Because the ASTER imagery was able to recreate the glacier boundary with 5% error, we assume that all debris-free ice will be mapped with the same uncertainty.

2.6 Results

To update the glacier inventory and quantify area change, the outdated USGS baseline was compared to the recent ASTER inventory. The USGS inventory contains a total of 1615 snow and ice bodies that account for 291.9 ± 2.2 km^2. Those same features account for only 232.3 ± 11.6 km^2 in the updated ASTER inventory, a 20% decrease in area. This aggregate area reduction shows that the outdated USGS maps do not represent

current glacier coverage. Due to complications from inconsistent inventory survey dates, we are concerned with local glacier characteristics (Table 2.3) as map dates are locally consistent.

Occupying low altitudes, NOCA glaciers account for a considerable portion of regional ice cover. The USGS inventory from Granshaw (2002) contains only snow and ice bodies >0.1 km^2 as mapped by Post *et al.* (1971), and we therefore consider the area estimates presented here as a minimum. Approximately 16% of glacier area was lost in the 48 years between 1958 and 2006, updating total glacier cover to 99.0 ± 5.0 km^2. This area estimate is less than the 1998 estimate from Granshaw and Fountain (2006) of 109.1 ± 1.1 km^2. The NOCA is also home to the majority of large glaciers (> 0.1 km^2).

Glaciers in the Olympic Mountains have changed the least of the three sub-regions even though they inhabit the lowest mean elevation. From 1987 to 2004, only a 1% decrease in area was observed, resulting in the smallest rate of ice loss. Our updated 2004 ASTER inventory shows total snow and ice cover of 37.3 ± 1.9 km^2. Although mostly attributed to large glaciers (29.4 ± 1.5 km^2), the small features are significant in number accounting for just over 20% of total ice cover.

When aggregated, glaciers on the Cascade Volcanoes have experienced the largest area loss with local variations. The glaciers of Mount Rainier and Mount Jefferson have low ice loss rates, comparable with North Cascades glaciers. Mount Hood on the other hand has experienced a 67% decrease in ice cover from 1956 to 2003 at a rate over 4 times that of the North Cascades. Altogether these glaciers comprise 96.0 ± 4.8 km^2 of the updated ASTER inventory. Mount Rainier alone accounts for nearly 70% of total glacier cover. As expected, large glaciers on Cascade Volcanoes did not experience as much loss as the small features.

Although we present ASTER results from a single year for each Cascade Volcano in Table 2.3, significant fluctuations in area are visible on a year to year basis. Table 2.4 shows ice area calculations on Mount Adams from five different ASTER images in addition to the USGS inventory. Depending on the year selected, a variety of area

Table 2.3: Local and Regional Snow and Ice Body Characteristics

	Elevation (m)			ALL				LARGE FEATURES ONLY[1]			
	Min	Max	Mean	#	USGS (km^2)	ASTER (km^2)	% Change	#	USGS (km^2)	ASTER (km^2)	% Change
North Cascades[2]	**1085**	**2720**	**2025**	**321**	**117.3 ± 1.0**	**99.0 ± 5.0**	**-16 ± 4**	**221**	**111.5 ± 1.0**	**94.0 ± 4.7**	**-16 ± 4**
Olympics	**1080**	**2405**	**1765**	**383**	**37.5 ± 0.6**	**37.3 ± 1.9**	**-1 ± 5**	**45**	**30.2 ± 0.6**	**29.4 ± 1.5**	**-3 ± 5**
Cascade Volcanoes	**1405**	**4395**	**2540**	**911**	**137.4 ± 1.8**	**96.0 ± 4.8**	**-30 ± 4**	**82**	**125.7 ± 1.7**	**93.4 ± 4.7**	**-26 ± 4**
Rainier	1450	4395	2700	431	78.0 ± 1.3	66.7 ± 3.3	-14 ± 5	38	74.1 ± 1.3	66.0 ± 3.3	-11 ± 5
Adams	1970	3745	2720	163	19.1 ± 0.7	11.1 ± 0.6	-42 ± 5	17	17.4 ± 0.7	10.7 ± 0.5	-39 ± 5
Hood	1405	3420	2320	125	21.9 ± 0.8	7.2 ± 0.4	-67 ± 4	25	19.7 ± 0.8	7.1 ± 0.4	-64 ± 5
Jefferson	1895	3175	2470	36	5.6 ± 0.3	4.4 ± 0.2	-21 ± 6	7	4.8 ± 0.3	3.9 ± 0.2	-17 ± 8
Three Sisters	2050	3150	2480	156	12.8 ± 0.4	6.6 ± 0.3	-48 ± 4	30	9.7 ± 0.4	5.7 ± 0.3	-41 ± 5
TOTAL				**1615**	**291.9 ± 2.2**	**232.3 ± 11.6**	**-20 ± 4**	**348**	**267.4 ± 2.2**	**216.8 ± 10.9**	**-19 ± 4**

[1] Characteristics for glaciers > 0.1 km^2 only

[2] Glacier boundary data from Granshaw (2007). Snow and ice bodies were filtered to match the inventory by Post *et al.* (1971) and as a result not all features delineated on the USGS maps are included.

estimates can be obtained. For our ASTER inventory (Table 2.3), we chose the smallest ASTER area calculation since it most likely represents *permanent* snow and ice features. Table 2.4 shows that by 2005, most small features were eliminated. We assume that reduction results from the removal of transient snow pockets. South Cascade net balance data in Figure 2.4 support that assumption. Multiple positive balance years in the late 1990s allow for transient snow patches to persist from year to year, resulting in the large area estimate seen at Mount Adams in 2000. The subsequent series of negative balance years removed all these bodies, leaving behind glacier ice and permanent snowfields. These variations should be considered when creating glacier inventories from satellite imagery.

Table 2.4: Area Calculations for Mount Adams, WA

Year	Date	All Features (km^2)	Large Features (km^2)	Small Features (km^2)
USGS				
1969		19.1 ± 0.7	17.4 ± 0.7	1.7
ASTER				
2000	09/25	21.6 ± 1.1	19.5 ± 1.0	2.1
2002	09/24	15.2 ± 0.8	14.0 ± 0.7	1.2
2003	09/27	14.7 ± 0.7	13.7 ± 0.7	1.0
2005	09/07	11.1 ± 0.6	10.7 ± 0.5	0.4
2006	09/10	15.5 ± 0.8	14.3 ± 0.7	1.2

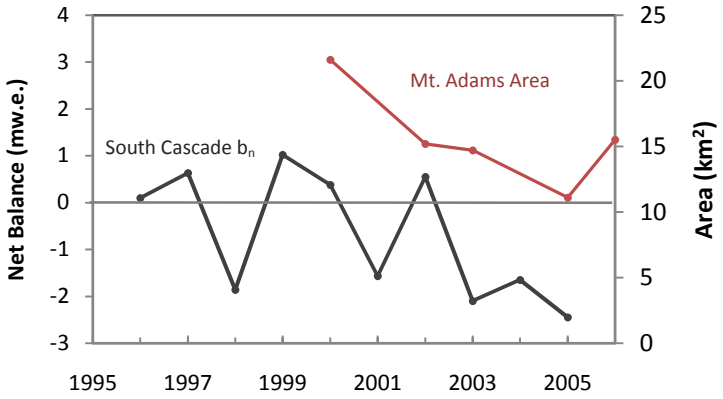

Figure 2.4: Net mass balance at South Cascade Glacier and Mt. Adams ASTER area calculations from 1996 to 2005 (Bidlake *et al.*, 2006). The late 1990s are dominated by positive balance years, whereas negative balance years are prominent in the 2000s. The smallest area calculation occurs after a series of negative balance years.

2.7 Discussion and Conclusion

Using ASTER satellite imagery, glacier cover was updated for much of the Pacific Northwest. In the 2000s, total snow and ice cover for our study area is 232.3 ± 11.6 km^2, which is 20% less than equivalent glacial features mapped from USGS topographic maps. Even though the USGS maps used vary in production date, they are not representative of current land cover in the mountainous Pacific Northwest.

In fact, only glaciers of the Olympic Mountains show insignificant change since their USGS map production date. Interestingly, the 37.3 ± 1.9 km^2 of snow and ice cover the lowest elevations yet has been shrinking the slowest. We surmise that because of their proximity to the coast, these snow and ice bodies consistently receive enough winter accumulation allowing them to persist year-to-year, whereas the remaining features are much farther from the coast resulting in a more variable accumulation pattern. Creating multiple inventories from multiple years would give us confidence in whether our inventory is actually representative of permanent features only.

Our 2006 North Cascades ASTER inventory contains 99.0 ± 5.0 km^2 of snow and ice and indicates a 16% area loss from the 1958 USGS maps. Similar to the Olympics, results from more years would improve actual estimation of permanent features. Granshaw and Fountain (2006) calculated a 7% reduction in glacier area from 1958 to 1998, which indicates our estimate is reasonable assuming the features have been shrinking since 1998. South Cascade Glacier, south of the Park, exhibits that pattern. Therefore, the 16% area loss is realistic, indicating these bodies have experienced more retreat since their USGS mapping than those in the Olympics.

The remaining 96.0 ± 4.8 km^2 of snow and ice features are found on the lofty summits of the Cascade Volcanoes and are rapidly retreating in comparison to the rest of the region. As a whole, these mountains have lost 30% of their original USGS snow and ice cover. Debris-free ice on Mount Rainier has been shrinking at a rate comparable to that of the North Cascades. Mount Adams, Mount Hood, and the Three Sisters region to the south, however, have experienced the most rapid losses. Mount Hood alone has 67% less snow and ice cover in 2003 than its 1956 USGS coverage. Interestingly, Mount Jefferson features have been slowly retreating like those on Mount Rainier and in the North Cascades. We found smaller fractional area changes for large glaciers, which Granshaw and Fountain (2006) attributed to their smaller area-volume ratio.

These data must be interpreted with caution, as we are only assessing area at two points in time. Based on our results, we might assume glaciers of the Cascade Volcanoes have been shrinking more rapidly than those in both the Olympics and North Cascades. However, terminus fluctuations since 1901 on Mount Hood from Lillquist and Walker (2006) present a complicated glacial advance/retreat regime with decadal scale fluctuations. As a result, comparison of the fractional area change across two different time periods could be misleading. Therefore, this new inventory allows us to look at the current state of glacial cover in the region, but we are unable to make interpretations about climate-glacier interactions because of the lack of a consistent baseline date.

Our results from the Cascade Volcanoes highlight an important consideration when using remotely sensed data for monitoring changes in glacier area. On a year-to-year

basis, snow cover can fluctuate significantly. Persistent snowcover can obscure the calculated glacier area extent, so depending on the image year, variable estimates of glacier area can result. By estimating snow and ice cover for consecutive years, we are then able to select the results that most likely represent the *permanent* features. We surmise that obtaining a realistic estimate of perennial snow and ice features requires remotely sensed imagery that was acquired after negative balance years. Area results in the early 2000s are very high, which is most likely due to the persistence of snow that would not exist in a typical balance year. Since 2001 and 2003-2005 are negative balance years, only glacial ice and resistant snow bodies will remain at the end of the melt season. Therefore, when creating a glacier inventory from satellite imagery, consideration of the local recent mass balance history is important.

Chapter 3 – Second Manuscript

Model investigation of climate change impacts on glacier mass balance and geometry for four glaciers in the Pacific Northwest

3.1 Abstract

To investigate climate change impacts on four glaciers in the Pacific Northwest, we estimate the influence of natural climate variability on the mass balance of these glaciers and their sensitivity to climate perturbations. Model results under these perturbations are then used to determine potential glacier geometry changes. The precipitation temperature area-altitude (PTAA) balance model requires only precipitation, temperature, and glacier area-altitude distribution as inputs and is not reliant on direct mass balance measurements, providing a model suitable for application to multiple glaciers. A strong relationship ($r^2 = 0.83$) between modeled and measured balance from the calibration period at South Cascade Glacier validates model accuracy. Results from the four glaciers show a recent strengthening of the relationship with the El Niño/Southern Oscillation (ENSO) from the mid-1980s to the present. The correlation strengthening between ENSO and summer temperatures around 1985 is manifested in our results through enhanced summer melt. However, the influence of the Pacific Decadal Oscillation (PDO) on balance fluctuations is more ambiguous, as the recent 1976/77 shift into a warm phase is weakly distinguishable at only one study glacier.

Glacier sensitivity estimates for a 1° C rise in temperature range from -0.73 to -1.09 mw.e., decreasing with latitude; however, no discernible pattern of precipitation sensitivity exists. Results indicate that at South Cascade, a 30% increase in winter precipitation could offset a 1° C rise in temperature. Glaciers further south require a >40% increase in winter precipitation to remain in balance. However, South Cascade is the only glacier of the four that could not exist under a 2° C warming scenario as its accumulation area occupies very low elevations. We postulate that the sensitivity of South Cascade glacier does not change as rapidly as those of the remaining three glaciers as the glacier retreats, making it the most vulnerable to climate change.

3.2 Introduction

Glaciers and ice caps have significantly contributed to global sea level rise during the 20th century through mass loss (Ohmura, 2006; Raper and Braithwaite, 2006; Dyurgerov and Meier, 2005). Additionally, glacier mass balance influences regional freshwater availability affecting both local and regional hydroelectric production and water supply. To understand how climate change will potentially modify these impacts, knowledge of the interaction between climate and glacier mass balance is essential. Using *in situ* balance measurements as a basis, simple mass balance models are often used to investigate the effect of climate perturbations through sensitivity analysis (e.g., Schuler *et al.*, 2005; Klok and Oerlemans, 2004); however, regional patterns (i.e., application to more than one glacier in the region) are rarely investigated.

The primary objective of this study is to apply a simple mass balance model to multiple glaciers in the Pacific Northwest, USA to identify the influence of natural climate phenomena (i.e., PDO and ENSO) on glacier mass balance and calculate its sensitivity to realistic climate change scenarios. To investigate the physical impact of climate change, potential glacier geometry changes are also presented for two warming scenarios based on model output.

3.3 Importance of Regional Assessment

Studying glacier mass balance at multiple spatial scales is crucial for an improved understanding of where glaciers are experiencing changes in mass balance, what is controlling those changes, and how those changes in turn are going to affect the climate system. Investigations of individual glacier mass balance are important for determining local controls such as shading, avalanching, wind redistribution, hypsometry, etc. Unfortunately, extrapolating such balance variations over an entire region would be erroneous even though all glaciers might be equally influenced by climate dynamics. Letreguilly and Reynaud (1989; 1990) discovered the existence of both time dependent (result of climate) and independent (result of glacier hypsometry) components of a glacier mass balance, complicating spatial extrapolation. Walters and Meier (1989) take mass

balance data from six glaciers to describe variability for western North America, which could be validated through a regional assessment of glacier mass balance.

The Intergovernmental Panel on Climate Change (IPCC) (Lemke *et al.*, 2007) has declared the need for glacier monitoring on a regional scale to reduce uncertainties in estimated ice variability. Because global ice loss cannot be measured, extrapolation is required from available observations. For instance, Meier (1984) uses mass balance data from 25 glaciers representing 13 regions worldwide to make a *global* assessment of alpine glacier contribution to sea level rise. Just over twenty years later, Ohmura (2006) determined global mean mass balance using data from 75 glaciers representing 14 regions. However, a global study of glacier mass balance would be most effectual in determining glacier contribution to sea level rise if regional patterns were integrated.

This study compares simple mass balance model results for four glaciers across Northern Oregon and Washington to generate a more accurate depiction of regional scale impacts of climate change.

3.4 Glacier Setting

Home to hundreds of alpine glaciers of various sizes, the northwestern U.S. is experiencing glacier mass loss at one of the fastest rates across the globe (Dyurgerov and Meier, 2005). For an updated inventory of the glaciers in the Pacific Northwest (PNW), see Chapter 2. Perennial snow/ice cover is shown in Figure 3.1 as well as the location of our four study glaciers, which are presented and described in Table 3.1.

Located in the North Cascade mountains of Washington state, South Cascade glacier is part of the U.S. Geological Survey (USGS) Glacier Monitoring Program, devoted to developing an understanding between glaciers and climate. Each USGS benchmark glacier is characterized by a series of field measurements, including glacier mass balance. For South Cascade glacier, balance measurements are available from 1959-2005 (Bidlake *et al*., 2007), including the winter and summer components. The glacier is incorporated in this study for model validation in addition to the study objectives. Tahoma, White River, and Jefferson Park glaciers cling to high volcanoes of the Cascade Range and do

not have balance measurements. These glaciers were selected because of their minimal debris cover to represent glaciers on the Cascade volcanoes.

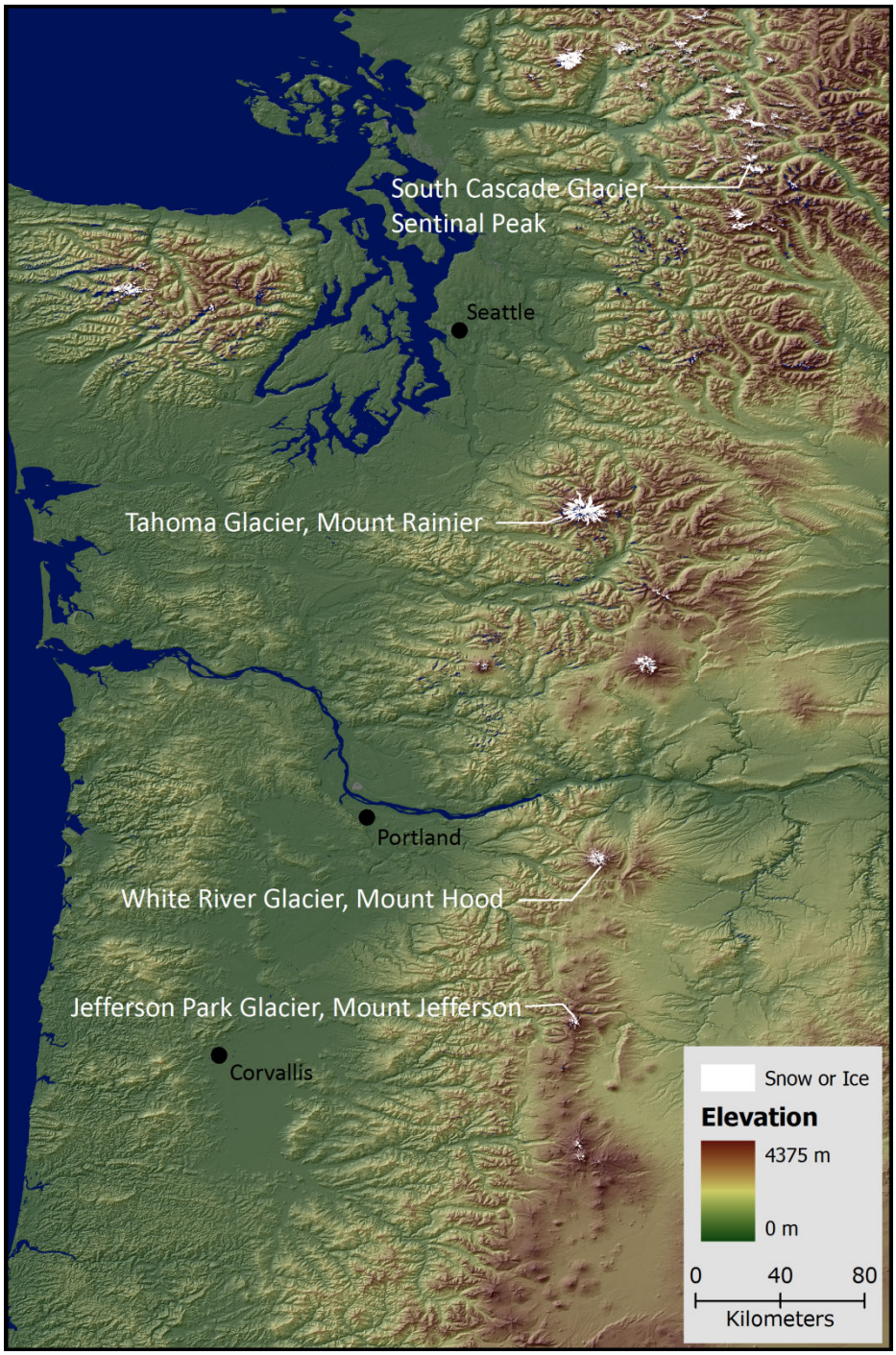

Figure 3.1: Study glaciers shown relative to PNW topography. Perennial snow/ice bodies are also outlined.

Table 3.1: Modeled glacier characteristics

Glacier	Latitude	Longitude	Slope (deg)	Aspect (deg)	Elevation (m)			Area (km^2)
					Min	Max	Mean	
South Cascade	48° 22' N	121° 04' W	14	295	1635	2125	1925	1.88
Tahoma	46° 50' N	121° 49' W	23	245	1845	4355	2925	6.39
White River	45° 21' N	121° 42' W	25	165	2115	3095	2525	0.38
Jefferson Park	44° 41' N	121° 49' W	25	320	2215	2915	2515	0.50

3.5 Climate Setting

To approximately represent climate conditions near these glaciers, we summarize data recovered at the Paradise (1560 masl) SNOTEL site on Mount Rainier, Washington from 1990 – 2006. At Paradise, nearly 2300 mm of precipitation falls in the winter, approximately 75% of annual precipitation. The average annual temperature is 3.6°C with an average winter temperature of -0.6°C. Annual deviations result from internal climate variability as well as two regional climate phenomena: the Pacific Decadal Oscillation (PDO) and the El Niño/Southern Oscillation (ENSO) (Mantua and Hare, 2002; Gershunov and Barnett, 1998).

3.5.1 Pacific Decadal Oscillation

A governing force in PNW decadal scale climate variability, the PDO generates both surface precipitation and temperature anomalies. Shifting every 20-30 years, the PDO phase is determined by the pattern of sea surface temperatures (SSTs) in the northern Pacific Ocean. During a warm phase, the northernmost Pacific experiences anomalously cool SSTs except along the northwest coast of North America where significantly warm SSTs prevail. Meteorological data used in this study encompass two warm phases (1927-1946, 1977-1999) and one cool phase (1947-1976) (Mantua and Hare, 2002). Due to the lack of understanding of this oscillation, the teleconnections are undefined (Mantua and Hare, 2002). Nevertheless, many studies have linked changes in surface climate with the PDO, and therefore, we investigate the existence of a potential relationship to glacier mass balance in the PNW. More specifically, a PDO warm (cool) phase brings warmer (cooler) and drier (wetter) winters on average to the PNW (Mantua and Hare, 2002). Beebee and Manga (2004) discovered a strong relationship between the PDO and date of

peak snowmelt and spring/summer runoff in Oregon, which also suggests comparison to glacier mass balance is suitable.

3.5.2 El Niño/Southern Oscillation

Similar to the PDO, ENSO variability is manifested in surface temperature and precipitation. Also characterized by SST anomalies in the Pacific Ocean, the strength and phase of ENSO is determined by the pressure gradient between the eastern and western equatorial Pacific, modifying the east-west SST gradient. During an El Niño event, the pressure gradient is weakened and warmer SSTs remain in the eastern equatorial Pacific. Such modification of the SST pattern ultimately affects the atmosphere above, connecting this oceanic phenomenon with the land surface. The PNW experiences a drier (wetter) and warmer (cooler) winter during a typical El Niño (La Niña) event (Miles *et al.*, 2000). Although their surface manifestations are similar, ENSO phase duration is much shorter (1-3 years) than the PDO (An and Wang, 2000).

The climate impacts of ENSO are well understood and its relationship has been tested against hydrologic and climate variables in the region. Beebee and Manga (2004) show a strong correlation between ENSO and annual discharge in Oregon streams. Redmond and Koch (1991) find no ENSO correlation with summer variables but that El Niño events typically bring below average winter precipitation and temperature to the high Cascades of Oregon and Washington. They also stress that snow accumulation may be influenced by the combination of winter precipitation and temperature anomalies in our study region associated with ENSO. Francou *et al*. (2004) found strong evidence linking glacier ablation to ENSO in the Andes of Ecuador, further leading us to consider the influence in the PNW.

This study uses results from a simple mass balance model to investigate the relationship between the ENSO and PDO and mass balance of four glaciers in the Pacific Northwest. Additionally, we calculate glacier sensitivity to multiple climate scenarios and estimate possible glacier geometry changes under select temperature change scenarios.

3.6 Data Sources

In order to validate model output, we compare our simulated results for South Cascade glacier with those measured by the USGS Glacier Monitoring Program. Values for winter, summer, and net balance between 1959 and 2005 were acquired from Bidlake *et al*. (2007). Objectively determined error associated with balance measurements is not published but assumed as a few tenths of a meter. Krimmel (1999) uses an error estimate of 0.20 m for net balance at South Cascade based on his comparison with geodetic balance results. Such a large estimate highlights the need to take caution when comparing our model results with these balance observations. Because of the difficulty to make precise balance measurements, the ability to create a model that near-perfectly reproduces actual observations is extremely difficult. In fact, a model that is capable of such a feat might not correctly capture the influence of climate on mass balance.

Glacier hypsometry (size and altitude distribution) was determined using recent Advanced Spaceborne Thermal Emission and Reflection Radiometer (ASTER) satellite imagery and a digital elevation model (DEM). ASTER Level 3 orthorectified images and the DEM were obtained from the Land Processes Distributed Active Archive Center at the National Aeronautics and Space Administration (NASA, 2007) for each glacier near the end of the water year (October 1). Radiance images used have either 15 or 30 m spatial resolution depending on spectral band, and the DEM has 30 m resolution with an accuracy of <25 m RMSE in all three dimensions. For an explanation of actual glacier delineation, see Chapter 2; the method is capable, mapping South Cascade glacier with an average error of 5%.

Temperature and precipitation data proximal to the study glaciers were acquired for seven meteorological stations in Washington and Oregon from the National Climatic Data Center (NCDC, 2007). Table 3.2 summarizes station characteristics. Values of the Mantua (2008) PDO index were used for years 1927-2006. This standardized index is calculated as the leading principal component of monthly SST variability in the Northern Pacific. The Multivariate ENSO Index (MEI) developed by Wolter and Timlin (1993) and available through the Comprehensive Ocean-Atmosphere Data Set at the National

Oceanic & Atmospheric Administration (NOAA, 2008) is based on six different measurable variables over the tropical Pacific, including sea-level pressure. We used fall and winter MEI values from 1950 to 2006. Also, seasonal values of the Southern Oscillation Index (SOI) from the Climate Prediction Center at NOAA (2008) were used. SOI values are based solely on sea-level pressure anomalies in the South Pacific.

Table 3.2: Meteorological stations

Station Name	COOP ID	Period of Record	No. of Years	Gage Elevation (m)	Data*	Glacier	Dist. To Glacier (km)
Diablo Dam	452157	1935 - 2006	72	272	T, P	SC	3.9
Concrete	451679	1935 - 2006	72	59	P	SC	5.5
Longmire	456894	1950 - 2005	56	842	T, P	T	0.9
Randle	456909	1950 - 2005	56	274	P	T	3.4
Three Lynx	358466	1927 - 2006	80	341	T, P	WR, JP	3.8
Estacada	352693	1927 - 2006	80	137	P	WR	4.8, 5.3
Detroit Dam	352292	1959 - 2006	48	372	P	JP	3.5

* Indicates whether temperature (T), precipitation (P) or both were acquired

3.7 Glacier Mass Balance Model

This study relies on a relatively simple model of glacier mass balance developed by Tangborn (1999) called the Precipitation, Temperature, and glacier Area Altitude (PTAA) model. By exploiting the links between climate, mass balance, and erosion, the PTAA model reconstructs glacier mass balance using only precipitation, temperature, and glacier hypsometry as inputs (Tangborn, 1999; Wood, 2006; Zhang *et al*., 2007). Similar to temperature index models, inputs are few and easy to attain, the calculations are straightforward, and glacier climate sensitivity can be assessed. Most importantly, the PTAA is not reliant on direct mass balance measurements and is still capable of producing realistic balance calculations, constructing a competent model that can be applied to any glacier as long as nearby climate data exist. The PTAA model has been proven capable through its ability to recreate mass balance observations over a wide range of glaciers including those in the North Cascades of Washington (Tangborn, 1999; Wood, 2006), Gulkana (Zhang *et al.,* 2007), Hubbard and Bering Glaciers (Bhatt *et al*., 2007) in Alaska, and Langtang Glacier in Nepal (Tangborn and Rana, 2002).

3.7.1 Input Data

3.7.1.1 Meteorological Data

This study relies on proximal stations to recreate climate conditions at the glacier. Long term daily maximum and minimum temperatures and daily precipitation observations were acquired from several low altitude stations <10 km from the glacier. Although data collected at the glacier are preferred, such records do not exist other than for South Cascade glacier in the PNW. Many modeling studies have shown that these low altitude stations are capable of generating realistic results (e.g., Braithwaite and Zhang, 1999; Tangborn, 1999; Klok and Oerlemans, 2004; Schuler *et al.*, 2005). Stations were selected not only based on their proximity to the glacier but also on the length and reliability of the record. Days without any observations were assigned a value based on the regression relationship with observations at a nearby station. Stations possessing extended intervals of missing or incomplete data were not used.

3.7.1.2 Area Altitude Profile

The hypsometry, or altitudinal distribution of glacier area, is an important control on the mass balance of a glacier (Furbish and Andrews, 1984; Tangborn *et al.*, 1990). A glacier that is in equilibrium under a constant climate is divided by the equilibrium line altitude (ELA) in such a way that all snow accumulated above the ELA is equivalent to the ice ablated below. Modifying glacier shape or altitudinal distribution will change the mass balance even without a change in the ELA. If one imagines sliding the balanced glacier down slope into a lower altitude range, it is easy to visualize that glacier area is lost above the ELA and gained below (remember the ELA will be fixed in a constant climate). The glacier is now in disequilibrium as the snow accumulated above the ELA will not be able to compensate that lost below. It is therefore important to consider changes in climate as well as changes in the area altitude distribution of a glacier in order to construct an accurate representation of glacier mass balance.

Because this study is primarily interested in calculating glacier climate sensitivity, only a recent area altitude profile is used in the model runs. By modeling balance fluctuations using the current area altitude distribution, we can impose climate

perturbations and observe the resulting mass balance changes to understand current glacier sensitivity to such scenarios. This static sensitivity determines the effect of climate change on a *specific* glacier area distribution and does not incorporate the influence of ice dynamics. Braithwaite and Zhang (1999) describe in detail the difference between the static and dynamic sensitivity of glacier mass balance. Although the *dynamic* sensitivity provides a more comprehensive picture of the relationship between climate and glacier mass balance, the *static* sensitivity characterizes the principal climate control on mass balance. Furthermore, alpine glaciers can be highly dynamic, constantly changing in shape and size, and are difficult to monitor frequently and consistently. To incorporate such dynamics into the model would require modification of the area altitude profile annually or possibly more frequently. Such measurements simply do not exist for these glaciers.

Although the USGS has published topographic maps providing both glacier extent and surface topography, they are not suitable for a study interested in the current climate controls on mass balance because in many cases they were produced several decades ago (up to 50+ years). Comparing topographic surveys, Bidlake *et al.* (2007) discovered that South Cascade Glacier shrank about 35% in size from 2.71 km^2 in 1958 to 1.75 km^2 in 2005. Furthermore, Granshaw and Fountain (2006) calculated a 7% reduction of glaciated area in the North Cascades National Park Complex from 1958 to 1998 with a large variety of individual glacier changes ranging between +10.3% to -100%. The distinct changes in glacier size over 40+ years indicate that the outdated USGS topographic maps would not accurately represent current glacier conditions.

Area altitude profiles were instead determined from ASTER satellite imagery and are presented in Figure 3.2. The ASTER satellite provided data at a high spatial resolution (15-30 m) as well as a co-registered digital elevation model (DEM) of 30 m spatial resolution. The updated glacier boundaries were determined using an algorithm that relies on variations in the spectral reflectance of snow and glacier ice across the visible and shortwave infrared portions of the electromagnetic spectrum (Dozier, 1987). Compared with rock, soil, and vegetation, snow and ice are highly reflective in the visible parts of the spectrum but relatively dark in the shortwave infrared. Thus, they can be

readily distinguished for effective mapping. For the complete description of glacier mapping using ASTER imagery see Chapter 2**.** Using the ASTER DEM and the updated glacier boundary, a new area altitude profile was created for each of the glaciers. The fraction of glaciated area was calculated at even intervals of 60 m.

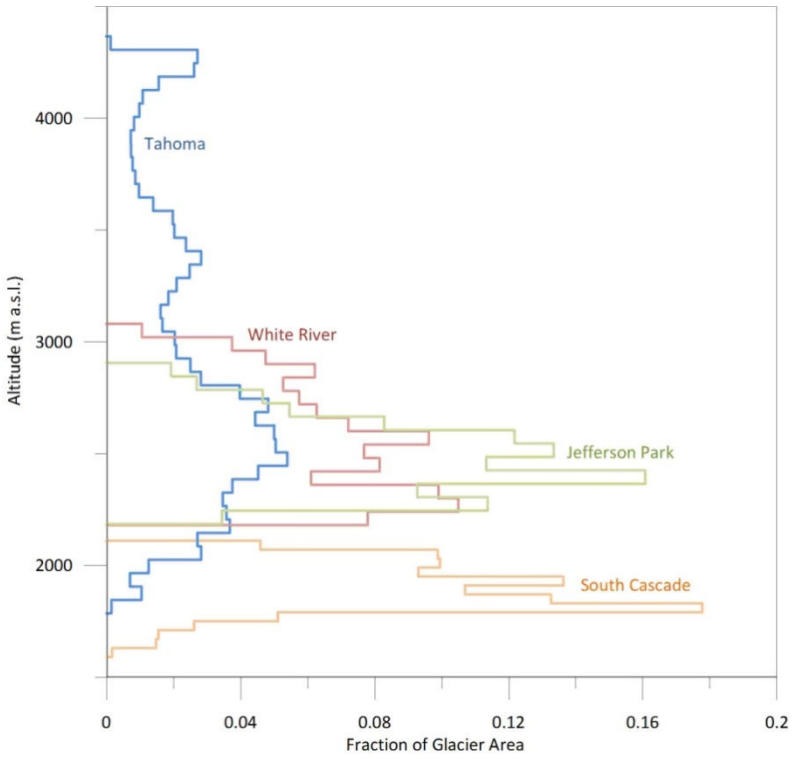

Figure 3.2: The unique area-altitude profiles for each study glacier. Each vertical step represents 60 m. Tahoma glacier area has a wide vertical spread incorporating both high and low elevations, whereas the narrow distribution for South Cascade is concentrated in the lowest elevations. Nearly similar in distribution, White River exists at slightly higher elevations than Jefferson Park glacier.

3.7.2 Model Description

The PTAA model is nearly self-reliant as it takes advantage of the unique relationship between climate, mass balance, and glacier hypsometry to calibrate its fifteen parameters. Energy balance as well as temperature-index models often rely on *in situ* measurements of mass balance in order to constrain coefficient values (e.g., Laumann and Reeh, 1993; Arnold *et al.*, 1996; Braithwaite and Zhang, 1999; Schuler *et al*., 2005). Hock (2003) notes that the degree day factor (melt factor) used in temperature-index models is highly

variable in both time and space, making it extremely difficult to constrain to a single value. Improvement in modeling the degree day factor would require more input data, adding complexity to an otherwise simple model. The model presented employs the simplex optimization technique (see section 3.7.3) to calibrate model parameters.

Fifteen model coefficients are used to convert air temperature and precipitation into accumulation and ablation at each altitude interval on the glacier and are described in Table 3.3. Eight balance variables are calculated daily, forming the basis of model calibration. The balance variables include:

1. Accumulation Balance (mw.e.)
2. Maximum Balance (mw.e.)
3. Minimum Balance (mw.e.)
4. Total Balance (mw.e.)
5. Accumulation Area Ratio (dimensionless)
6. Snowline Altitude (masl)
7. Zero Balance Altitude (masl)
8. Balance Flux (mw.e.).

Obtaining the optimized calibration coefficients is an iterative process. The model calculates balance variables using an initial set of coefficients and the model input data. A series of linear regressions are then created for different combinations of balance variables listed above for each day in the ablation season. The coefficient of variation (r^2) is determined for each regression, and the average r^2 is then attributed to that unique set of coefficients. The model is iteratively run with a different set of coefficients until a maximum r^2 has been reached producing the optimized set of coefficients. In other words, the model assumes a linear relationship between the balance variables, which can be exploited to determine optimal model coefficients. Tangborn (1999) makes both linear and non-linear regressions; however, results from the linear regressions do not deviate significantly from the non-linear.

Table 3.3: Model coefficients for each study glacier

No.	Description	Value			
		SC	T	WR	JP
C_1	Precipitation mulitplier at maximum altitude	2.172	1.888	1.990	1.601
C_2	Precipitation multiplier at terminus	1.080	1.217	1.038	1.143
C_3	Altitude of maximum precipitation	2050	3245	2883	2475
C_4	Precipitation station mixing fraction	0.511	0.625	0.922	0.886
C_5	Lapse rate intercept (above average temperature)	0.483	0.466	0.538	0.521
C_6	Lapse rate line slope (above average temperature)	0.00578	0.00475	0.00294	0.00495
C_7	Lapse rate intercept (below average temperature)	0.636	0.434	0.656	0.616
C_8	Lapse rate line slope (below average temperature)	0.00222	0.00690	0.00190	0.00221
C_9	Ablation from temperature (without precipitation)	0.00517	0.00775	0.00870	0.01080
C_{10}	Ablation from temperature (with precipitation)	0.01056	0.06497	0.05140	0.06180
C_{11}	Temperature melt threshold	0.163	0.178	0.188	0.111
C_{12}	Ablation from solar radiation	0.00039	0.00010	0.00098	0.00029
C_{13}	Seasonal snowline rise multiplier	20.146	50.171	79.336	37.900
C_{14}	Temporary snowline rise multiplier	202.226	287.477	519.574	260.246
C_{15}	Internal accumulation multiplier	3.551	5.089	6.607	7.540

3.7.2.1 Lapse Rate

The temperature at the glacier is an important control on both model ablation and accumulation; however, the input meteorological data consist of minimum and maximum daily temperatures at sites lower in elevation. The model calculates a daily lapse rate (°C m^{-1}) based on assumptions about the ambient conditions at the glacier and assigns a modified temperature to each altitude interval.

To more effectively simulate the temperature history at the glacier, four model coefficients (C_5-C_8) are used to vary the daily lapse rate. Table 3.3 shows that the minimum lapse rate for each of the glaciers ranges from 0.47-0.54 °C(100 m)$^{-1}$. The lapse rate is not constant in space and time, and in an attempt to capture some of that variability, the model considers two important controls on the lapse rate: cloudiness and the surface temperature. Temperature controls the moisture content of air and cloudiness is an indicator of saturation. The diurnal temperature range is used as an approximation of cloudiness with a large (small) range equivalent to a clear (cloudy) day. Furthermore, on days when the average temperature is higher than normal, the model assumes a parcel of air has the ability to retain more moisture limiting the amount of condensation that

occurs as that parcel rises. With little condensation, only a small amount of latent heat is released, allowing the parcel of air to cool more quickly. As a result, a hot/clear (cool/cloudy) day will have a high (low) lapse rate.

3.7.2.2 Accumulation

During the winter months, glaciers are experiencing a period of positive balance that results from the accumulation of snow. Two conditions must be met for snow accumulation at the glacier: (1) precipitation must be observed in the meteorological data and (2) the temperature must be at or below freezing (0°C). As a result, precipitation might fall as rain at the glacier terminus and snow at the glacier head, depending on the temperature at each altitude band.

Precipitation observations at low elevation stations must be manipulated to represent precipitation at the glacier. Due to the orographic effect on the saturation water vapor pressure, more precipitation will occur at the glacier (high altitude) than at the low altitude weather station. Precipitation is determined for each glacier altitude interval using three model coefficients: the precipitation multiplier at the terminus (C_2), the maximum precipitation multiplier (C_1), and the altitude of maximum precipitation(C_3). Generally speaking, precipitation across the surface of the glacier increases linearly from the terminus with elevation until it reaches a maximum and stabilizes. Accumulation occurs at a given altitude interval if it receives precipitation while the temperature is equal to or below freezing with a magnitude equal to the weighted gage precipitation results enhanced by the altitudinal multiplier. A fourth coefficient (C_4) determines the relative influence of the two input precipitation datasets. Such differentiation is important in order to potentially identify stations that are dependable and others that are not.

3.7.2.3 Ablation

Similar to a temperature-index model, ablation is induced by the daily temperature as well as the diurnal temperature range and a solar radiation component. Although melt results from the complex interaction of the energy balance components such as the net radiation, a strong relationship between melt and air temperature has been quantified

(Braithwaite and Olesen, 1989). Ohmura (2001) postulated that long-wave radiation and the sensible heat flux to a lesser degree are the dominant controls on melt and are highly regulated by air temperature. Because of this relationship, a turbulent heat transfer component of ablation reliant on air temperature is justified. Two coefficients regulate this component, differentiating melt on days with (C_{10}) and without rain (C_9). Furthermore, melt will only occur above a temperature threshold, determined by coefficient C_{11}, which ranges between 0.11 and 0.19 °C for each of the glaciers.

A second component of ablation simulates melt due to short-wave radiation (solar radiation), an important source of energy for melt (Ohmura, 2001). Albedo is a significant control on the solar radiation component of a glacier's surface energy balance, yet its effect is often inadequately parameterized in glacier mass balance models. Brock *et al*. (2000) describe the need for a more physical understanding of the spatial and temporal variability of glacier albedo, ranging in magnitude from <0.10 for ice and >0.90 for fresh snow. Although a more physically based approximation for albedo would undoubtedly create a more robust model, the addition of actual ground measurements would compromise model simplicity. Therefore, the model relates albedo to a varying snowline altitude using an ice ablation factor.

The snowline altitude is controlled by snow accumulation and ablation. The model assumes that the glacier above the snowline altitude is not experiencing any ablation from solar radiation. Although not entirely correct, the assumption highlights the idea that fresh snow is highly reflective, limiting the contribution of solar radiation to melt. This contribution increases with distance below the snowline. In the absence of fresh snow, this region contains low-albedo firn and ice of which the latter becomes completely dominant at the glacier terminus surface. The ice ablation factor captures these effects as a dimensionless variable analogous to surface albedo, determining the percent of solar radiation absorbed and available to produce melt. Above the snowline, the ice ablation factor is zero, and below, the factor increases linearly starting at the snowline altitude. During the winter months when the snowline is depressed below the glacier terminus, the entire glacier has an ice ablation factor of zero, and as a result solar radiation is not contributing to melt.

The short-wave component of melt is calculated using the ice ablation factor, a solar radiation index, the diurnal temperature range, which are converted into melt using model parameter C_{12}. The solar radiation index simply relates the day of the year to the relative magnitude of solar irradiance at a specific latitude. The diurnal temperature range is used once again as a proxy for cloudiness, and the model coefficient C_{12} converts the solar radiation index into actual melt.

Total ablation at each altitude interval is simply the addition of the turbulent heat transfer and the solar radiation components of ablation. Hence, melt can occur above the snowline altitude but only as a product of the turbulent heat fluxes.

3.7.2.4 Balance

Glacier mass balance is calculated at daily time steps at each altitude band using the accumulation and ablation algorithms described above. The balance at each altitude interval is simply the sum of total accumulation (+ mw.e.) and total ablation (- mw.e.). Although an understanding of the variation of mass balance with altitude is useful, in order to understand glacier health a comprehensive mass balance is calculated. Using the area altitude distribution of the glacier, the total mass balance is calculated through the summation of the altitude balances multiplied by the representative area fraction for each interval.

3.7.2.5 Other Balance Variables

Based on accumulation, ablation, and mass balance calculations, other glaciological characteristics are estimated as well. For instance, the snowline altitude either rises or falls daily based on accumulation and ablation. When the freezing level drops and snow falls below the current snowline, it is depressed to the freezing level. Melting snow then causes the snowline to begin to rise again. Additionally, the zero balance altitude (the division between areas of mass gain and mass loss), the accumulation area ratio, and the balance flux (mass flux across the zero balance altitude) are calculated as well. It is important to note that these variables are essentially constant during the accumulation (winter) season limiting the optimization regressions to the summer months only.

3.7.3 Calibration

To correctly convert low altitude temperature and precipitation into glacier mass balance, a set of fifteen coefficients is determined without "tuning" or using actual ground measurements. Instead, the coefficients are optimized using the Nelder-Mead Simplex Algorithm (Barton and Ivey, 1996).

Simplex optimization determines the set of parameters that minimizes a function of interest. In the case of the PTAA model, we are interested in maximizing the relationship between the calculated balance variables through the correlation coefficient (r^2). However, the Nelder-Mead Simplex algorithm attempts to minimize a function, so instead we will minimize the regression error or the complement of r^2 ($1 - r^2$). Nineteen linear regressions are made for each day of the ablation season. The length of the ablation season varies from year to year; however, assuming the season begins June 1st and ends September 30th (121 days), the optimization procedure will rely on 2,299 (121 days x 19 pairs) regressions. The nineteen linear regressions include:

1. Net Balance v. Zero Balance Altitude
2. Net Balance v. Snowline Altitude
3. Mass Flux v. Area Altitude Ratio
4. Net Balance v. Accumulation Balance
5. Maximum Balance v. Zero Balance Altitude
6. Maximum Balance v. Snowline Altitude
7. Maximum Balance v. Area Altitude Ratio
8. Area Altitude Ratio v. Zero Balance Altitude
9. Minimum Balance v. Snowline Altitude
10. Minimum Balance v. Zero Balance Altitude
11. Minimum Balance v. Area Altitude Ratio
12. Minimum Balance v. Mass Flux
13. Snowline Altitude v. Zero Balance Altitude
14. Zero Balance Altitude v. Area Altitude Ratio
15. Zero Balance Altitude v. Mass Flux
16. Snowline Altitude v. Area Altitude Ratio
17. Snowline Altitude v. Mass Flux
18. Area Altitude Ratio v. Mass Flux
19. Zero Balance Altitude v. Snowline Altitude.

The actual number of datapoints depends on the length of the record; each additional year adds a point to the regression. Not surprisingly, the longer the record, the more reliable the relationships and model results. Each glacier in our study has a calibration period between 1977 and 2006 indicating 30 data points are used in each regression. It is tempting to calibrate the model using the entire meteorological record; however, for reasons discussed later, this specific period was selected. Because the length of the ablation season is not fixed, regressions for days early in the ablation season might have fewer than the 30 pairs if the onset of melt was delayed.

The optimization process can most easily be illustrated using a simple thought experiment. Imagine a man trying to escape from a building on fire. That person is undoubtedly attempting to maximize his distance from the fire or minimize his distance from safety. When the fire alarm goes off, he quickly surveys the closest points of escape, noting whether they would bring him closer to fire or safety. Intuitively, he decides to head in the direction away from the fire in an attempt to minimize his distance from safety. He stops a moment to resurvey. His current path looks clear, so instead of creating a new escape route, he *expands* his distance from the fire and his area of safety. Eventually, he runs into more fire and decides to turn back, *contracting* his distance from the fire. Once he feels safe, he reassesses his escape routes, repeating the process until he *expands* his area of safety to encompass a reasonable exit and subsequently *contracts* his escape to a single point, the exit. The man has minimized his distance from safety using a mental simplex algorithm.

For the PTAA model, the mean of the complement of r^2 for all the regressions is minimized using the simplex optimization method. Like the man looking to move towards safety (away from fire), the model coefficients are moving to a point of the lowest error (or largest r^2). Because the model occupies a 15-dimensional space, human visualization of the optimization process is impossible. To initialize the model, sixteen (n +1) user defined parameter guesses or sets are run through the model, each producing a unique $1 - r^2$ value. Each of those initial guesses exists as nodes of a simplex in 15-dimensional space. Based on the distributions of the complement, the simplex is deformed iteratively through reflection, expansion, and contraction until the nodes all converge on a single point. At that point, the complement has been minimized and the optimal set of coefficients has been reached. However, the process often requires multiple runs of the simplex due to the large number of possible solutions that accompany such models. *A priori* knowledge of reasonable coefficients is necessary to produce realistic results. That is not to say that actual field measurements are required, instead a thorough understanding of the model and each of the coefficients is essential.

3.7.4 Sensitivity Analysis

To assess glacier climate sensitivity, additional model results from various climate perturbations were compared to those from the present climate, which is defined as the 1977-2006 average. In general, sensitivity is the difference between the average total mass balance under the present climate and the future climate scenario. Therefore, glacier sensitivity to climate change is expressed in units of mass balance per climate perturbation: e.g., mw.e. $°C^{-1}$, mw.e. $(10\%)^{-1}$. Perturbations include uniform modifications to the temperature input data and seasonal modifications to the precipitation input data. More specifically, six temperature scenarios were applied as the daily input data were perturbed in 0.5°C increments between -1.0°C and +2.0°C, incorporating a minor cooling and a range of warming scenarios. Four precipitation scenarios were created: ±10% and ±20% increase in winter precipitation (Oct. – Mar.). Results from the IPCC Report (Christensen *et* al., 2007) show that the Pacific Northwest can expect annual temperatures to rise by approximately 3° C and winter precipitation to increase about 10% by 2080-2099. Therefore, it is likely that our maximum temperature scenario of +2° C will be reached within the next century.

3.8 Comparison of Simulated Results and Observations

3.8.1 Previous Work

Although the PTAA model is capable of simulating the mass balance history for glaciers lacking actual field measurements, model assessment is crucial to instill user confidence in the results and also determine areas of potential improvement. In his first publication of the model, Tangborn (1999) completed the initial model assessment using South Cascade glacier. In comparison with direct measurements of mass balance at the glacier, simulated results explained 57% of the variance in the observed balance dataset with a RMSE of ± 0.75 mw.e. (Tangborn, 1999). Glacier mass balance measurements are not precise and often contain large error in both measurement and extrapolation. As a result, near perfect relationships between measured and simulated mass balance are

unattainable. Model capture of observed balance variance makes the PTAA model capable.

Subsequently, Wood (2006) tested the model by applying it to four glaciers in the North Cascades Park in Washington. The North Cascades Glacier Climate Project has monitored the annual balance of two of these glaciers (Easton and Rainbow) since 1990. The North Cascades National Park has monitored annual balance of the remaining two glaciers (Noisy and North Klawatti) since 1993. The fractions of the observed mass balance variance explained by the simulated results for each glacier are 0.44, 0.68, 0.71, and 0.84, but it should be noted that the relationships were based on a relatively small number of data points (from 12 to 20). Wood (2006) ultimately concluded that the model produced useful results for studies at a small scale, where precision is not imperative.

3.8.2 Model Performance – South Cascade Glacier

Parameter optimization using the simplex method is completely independent of *in situ* measurements of glacier mass balance. To determine the utility of the model for calculating glacier climate sensitivity, this study runs the model for South Cascade glacier using its 2003 area altitude distribution. This mass balance recalculation using the PTAA model at South Cascade is important because it uses only a single, *recent* area altitude profile for mass balance calculations, allowing the authors to determine the current climate sensitivity of the glacier under certain climate scenarios.

3.8.2.1 Parameter Calibration

Although Tangborn (1999) published optimized parameters for modeling the mass balance of South Cascade glacier using the PTAA model, those results are not used in this study for multiple reasons. First, the author calibrates the model using *multiple* (ten) area altitude profiles, none of which incorporate a recent profile. Because changes in glacier area are considered, some of the effects of glacier dynamics are included in the mass balance calculations. This effect ultimately should produce more accurate mass balance results; however, this study is interested in the *static* sensitivity of the glacier, so it is unnecessary and erroneous to include multiple profiles in calibration. Second, the period of calibration is between 1955 and 1996. Climatic controls on mass balance

fluctuate with climate such as changes in atmospheric circulation patterns. As a result, attempting to calibrate the PTAA model over a long time period would undoubtedly produce results that are not representative of reality. Using the mass balance patterns for South Cascade glacier presented in Jorsberger *et al.* (2007), the calibration time period for this study is set at 1977-2003. Third, the published results only include fourteen parameters, as it is an earlier model version. The model has been updated to include a fifteenth coefficient controlling internal accumulation, which affects the other parameters' control on the mass balance. For these reasons, the PTAA model was recalibrated for South Cascade glacier between 1977 and 2003 using only a recent area altitude profile. When the parameters are optimized, an average r^2 of 0.89 for the ~ 2,299 linear regressions is obtained.

3.8.2.2 Comparison with Measured Balance

For the 27 years of the calibration period between 1977 and 2003, there is a strong relationship ($r^2 = 0.83$) between the modeled and measured values of net balance (Figure 3.3). There does not seem to be any systematic bias as the slope of the linear regression between the modeled and measured balances is close to one. However, a major source of concern is the *y*-intercept of +0.28, indicating the modeled balances are on average 0.28 mw.e. *more positive* than those measured (given that the regression slope is nearly one). Although significant measurement errors do exist, this discrepancy might be explained by the simple fact that the model is using the recent area altitude profile from 2003.

Because South Cascade glacier has experienced steady retreat since 1958, the authors infer that glacier area in 2003 is less than in 1977. In fact, assuming a linear retreat, the glacier lost approximately 25% of its 1977 area by 2003, the majority from low elevation. Using a recent glacier profile to model mass balance for years in which the glacier had more area in the lower elevations would produce a more positive net balance. This idea is further supported when looking at the annual differences between the modeled and measured net balances in Figure 3.4. The average difference in 5-year bins decreases from 1977 to 2003, from 0.51 mw.e. to 0.09 mw.e., suggesting that the use of the recent 2003 area altitude profile accounts for much of the positive bias of the mass balance results. Therefore, the authors propose the model accurately recreates annual mass

balance fluctuations and the positive bias is primarily a product of using a recent area altitude profile. Since this study is interested in the present climate sensitivity, model capture of the effects of climate variations is crucial, whereas the bias should be nearly inconsequential.

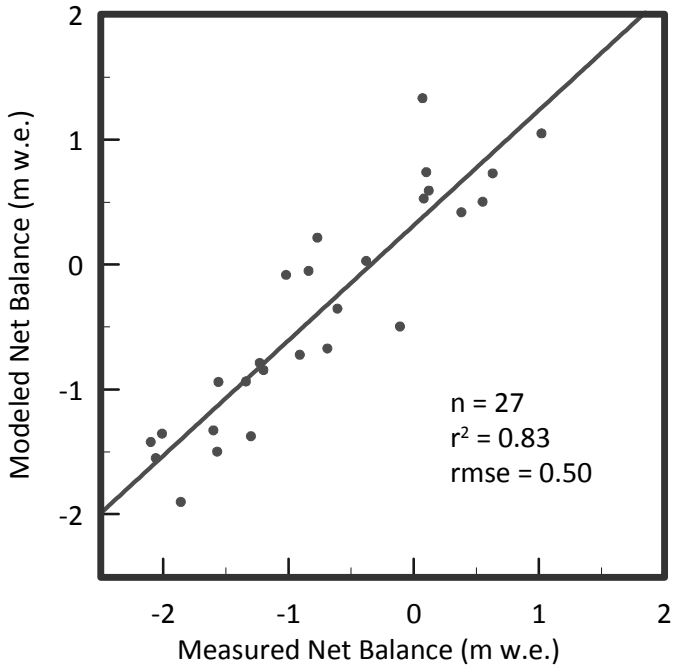

Figure 3.3: Model results for South Cascade glacier over the calibration period (1977-2003) compared to actual balance measurements. The best fit line based on the 27 data points has a slope of just less than 1 and a y-intercept of +0.28 mw.e., resulting in an r^2 = 0.83 and rmse = 0.50 mw.e.

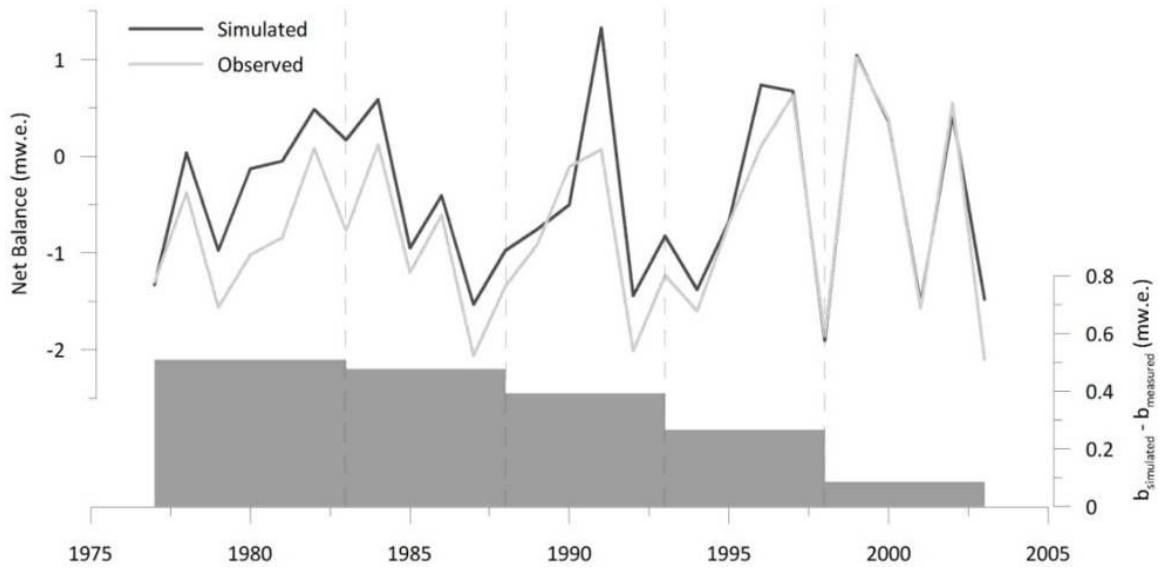

Figure 3.4: Net balance simulations and measurements during the calibration period (1977-2003). Bars represent the difference between simulated and measured results averaged in 5-year bins (first and last bins contain 6). The simulated results are more accurate later in the calibration period. The increase in the difference at towards the beginning of the period is most likely due to using the 2003 area-altitude profile. For instance, the 1977 profile would have more low altitude bands, decreasing net balance calculations. Annual variations are captured well.

As expected and visible in Figure 3.5a, applying the model to years excluded from the calibration period (1977-2003) results in a weaker relationship with mass balance observations. Model results from 1953-1976 yield an r^2 of 0.69, which indicates the model captures about 15% less of the variability in measurements as compared to the calibration period. Overall, the model is competent and captures a large amount of variability (75%) with a RMSE = 0.57 mw.e. (Figure 3.5b). Parameter calibration must take into account the idea that climatic influence on glacier mass balance changes with time. Therefore, model runs outside of the calibration period might not be able to capture the mass balance fluctuations completely because the climate controls were not modified to fit that climate regime. If the controls on mass balance were constant with time, model capture of variability should not change. Because the model is calibrated to a specific time period, climate sensitivity estimates only truly represent balance changes under the same regime. As a result, climate sensitivities are approximations of future mass balance changes with the assumption that no major climate shifts occur.

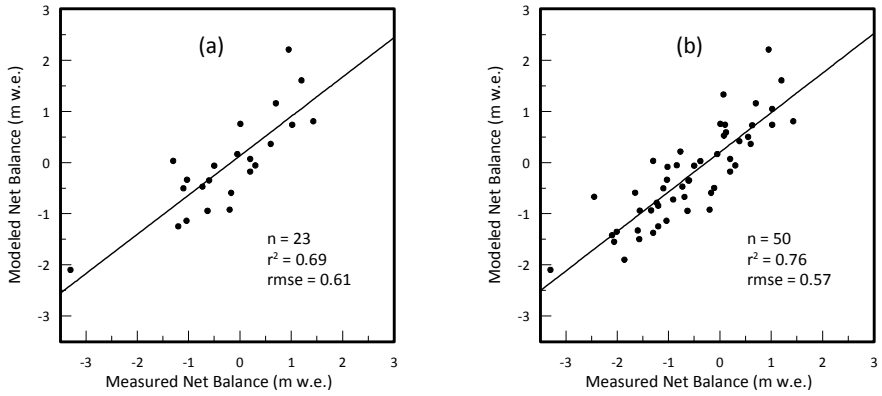

Figure 3.5: Comparison of measured net balance and (a) modeled result outside of the calibration period (1953-1976) and (b) all model results (1953-2003). Simulations prior to the calibration period are still capable of recreating mass balance with slightly more error. Considering the entire period, the model is able to capture ~75% of the variance in balance measurements.

3.9 Climate Trends and Mass Balance

Because the model is able to recreate mass balance fluctuations at South Cascade glacier employing a recent area altitude profile, the authors propose the model is similarly capable for use on other glaciers in the region lacking balance measurements. Results from unmeasured glaciers will allow for better assessment of regional glacier health. Although the model results have a positive bias, because mass balance variability is aptly captured, analyzing the simulated mass balance record highlights any relative trends and allows for a comparison between glaciers and changing climate phenomena.

Considering trends in the mass balance data series in Figure 3.6 might develop our understanding of their relationship with climate fluctuations. However, glacier balance is a function of complex climate relationships, making visual delineations of balance trends in Figure 3.6 difficult and subjective. A clear jump is noticeable in 1945, beginning a period of near neutral balance until the late-70s or even mid-80s, after which no simple classification can describe balance behavior. Therefore, instead of looking for trends in the balance data, we compare trends in two climate phenomena to balance fluctuations to resolve whether and how they relate.

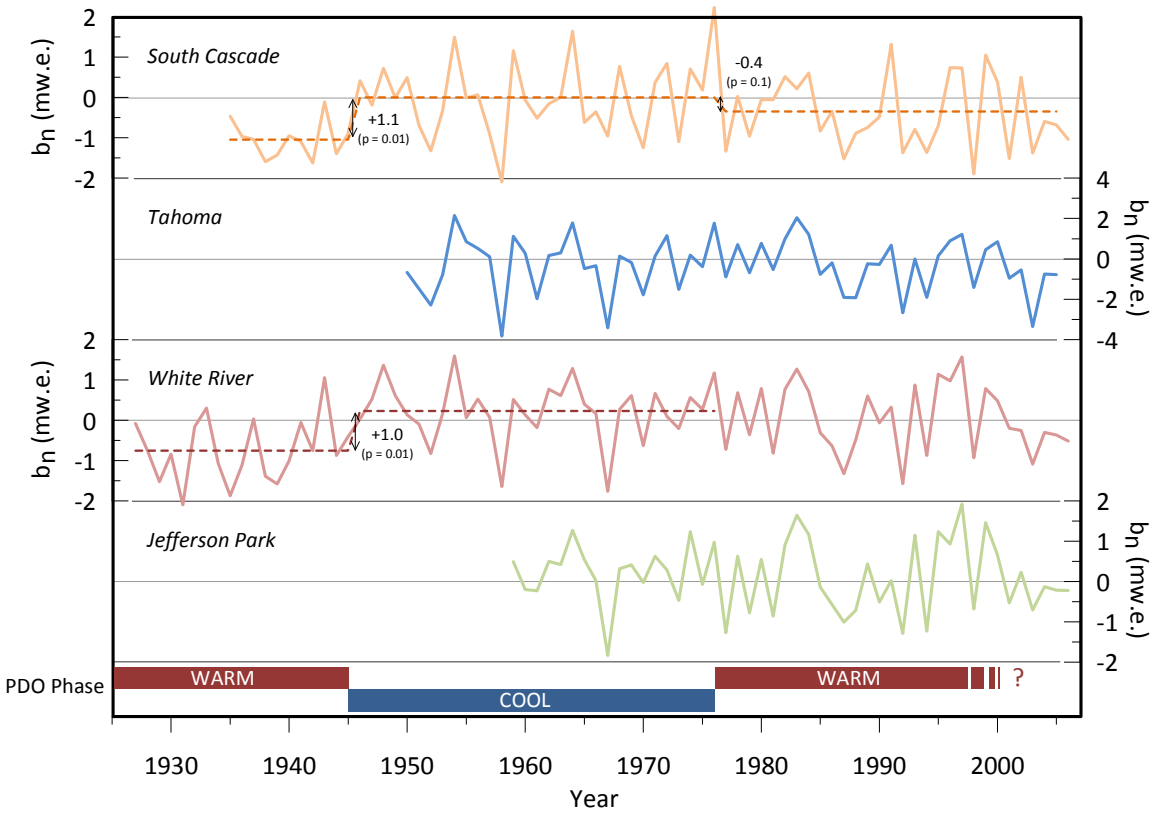

Figure 3.6: Simulated net balance time series for each study glacier. Phase transitions of the PDO are also presented; however, debate over a possible phase shift in the late-1990s prompted our uncertainty. Statistically significant jumps in average are also presented as dashed lines. Values beside the transitions are the magnitude of jump as well as the statistical p-value (p = 0.01 indicates a 99% probability that the shift is significant). Two balance transitions coinciding with phase shifts of the PDO occur at South Cascade glacier. Additionally, White River glacier experiences a balance transition during the 1944/45 PDO shift. The 1977/78 transition is not significantly manifested at Tahoma, White River, and Jefferson Park glaciers.

Our focus lies on the PDO and ENSO due to their influence on Washington and Oregon snowpack (Mote, 2006; Beebee and Manga, 2004) and temperature (Mote, 2006). We address the question of whether fluctuations in the phase and/or intensity of these oscillations are correlated with balance fluctuations for any or all of the study glaciers.

3.9.1 The Pacific Decadal Oscillation

Although studies have linked fluctuations in Northwest climate and hydrology to variations in the PDO (e.g., Redmond and Koch, 1991; Clark *et al.*, 2001; Kiffney *et al.*,

2002), results presented suggest either a decoupling or modification of this relationship in recent years. A long-term oscillation, the PDO generally exists in one of two phases that each persist for 20-30 years (Mantua *et al.*, 1997). Although inter-annual fluctuations are frequent in the 100+ year reconstruction of the PDO index, we analyze the mass balance characteristics during each of the two broad phases without emphasis on the influence of annual variation. Additionally, we only consider the time period between 1927 and 1997 due to uncertainty in the PDO phase beginning in 1998 (Beebee and Manga, 2004). As a result, our study incorporates one cold phase from 1946-1976 and two warm phases from 1927-1945 and 1977-1997.

To establish whether PDO phase and glacier mass balance are linked, we determine whether the balance mean in a warm PDO phase is statistically different from that in a cool phase. Put as a question: Can we confidently distinguish typical warm and cool phase balances from each other? Results in Table 3.4 show for both South Cascade and White River glaciers that significant differences in summer, winter, and net balances exist between the opposite PDO phases. However, Tahoma and Jefferson Park do not exhibit the same relationship, which might be a result of their record brevity. South Cascade and White River typically experience more negative (positive) winter, summer, and net balances during the warm (cool) PDO phase. Interestingly, the net balance during a warm phase is typically more negative by > 0.5 mw.e. than during a cool phase for both glaciers; South Cascade winter balance responds more intensely than its summer balance, the opposite of White River glacier.

Table 3.4: Average difference between warm and cool PDO phase balance

Glacier	**$\mu_{warm} - \mu_{cool}$ (mw.e.)**		
(pop.)	**b_w**	**b_s**	**b_n**
SC (n=63)	-0.35**	-0.24*	-0.59***
T (n=48)	-0.17	0.32	0.16
WR (n=71)	-0.23**	-0.30*	-0.53***
JP (n=39)	-0.08	-0.05	-0.13

Note: Triple asterisk (***), double asterisk (**), and asterisk (*) represent >99%, >95%, and >90% confidence respectively.

However, when we examine each phase shift separately, balance correlation with PDO phase is more ambiguous. Previously, balances were categorized into two bins: those from warm and those from cool phases. This method assessed the relationship over the entire record, ignoring possible changes over time. Therefore, balances are now categorized into three bins: those from 1927-45, 1946-76, and 1977-97. This method highlights any changes in the link between the PDO and net balance and its components, as we can determine whether any change in the balance average between bins is significant. The 1945/46 PDO shift from warm to cool phase coincides with a significant jump in net balance mean for both South Cascade and White River glaciers (Table 3.5). However, only South Cascade experiences a weak shift at the 1976/77 transition from a cool to warm phase. The remaining glaciers have indistinguishable balance means between 1946-76 and 1977-97, resulting in no balance shift. By grouping balance results by individual PDO phases, temporal and spatial variations are more apparent.

Table 3.5: Average balance differences (mw.e.) between individual PDO phase periods

Glacier	1944/45 Shift: W → C (mw.e.)			1976/77 Shift: C → W (mw.e.)		
	b_w	b_s	b_n	b_w	b_s	b_n
SC	0.73***	0.33**	1.1***	-0.16	-0.19	-0.35*
T	--	--	--	-0.17	0.32	0.16
WR	0.32***	0.66***	1.0***	-0.14	-0.03	-0.11
JP	--	--	--	-0.08	-0.05	-0.13

Note: Values are mean differences before and after phase shift. Triple asterisk (***), double asterisk (**), and asterisk (*) represent >99%, >95%, and >90% confidence respectively.

Based on these results, we infer that although a significant difference in balance is observed between warm and cool PDO phases for South Cascade and White River glaciers, the fact that no significant shift is observed at the 1976/77 transition back into a warm phase for all glaciers indicates the only South Cascade glacier remains linked to PDO phase. White River glacier (in addition to Tahoma and Jefferson Park) may have once been linked to PDO phase, as evidenced in the 1945/46 phase transition. However, their records only span 1 or 2 phase transitions, making inference about their relationship with PDO phase trivial. Because South Cascade glacier witnesses two phase transitions, both of which are accompanied by statistically significant shifts in mass balance, we infer

that the glacier is linked to the PDO, the strength of which is declining. When/If the PDO shifts back into a cool phase, South Cascade glacier might receive slightly more winter accumulation from more winter precipitation and/or lower winter temperatures and less summer ablation from a decrease in summer temperature. The link might eventually be broken, as is the possible case of White River and even Tahoma and Jefferson Park glaciers, making presumptions about mass balance after future phase transitions highly questionable. Perhaps this decoupling began with the glaciers to the south and is moving northward with time. Regardless, we postulate that the PDO might have once influenced glacier mass balance in the PNW; however, there is little evidence to support a continuing relationship except at South Cascade glacier where the correlation shows signs of weakening.

3.9.2 The El Niño/Southern Oscillation

Like the PDO, the effects of ENSO on snowpack and temperature in the PNW are of great concern (Ropelewski and Halpert, 1986; Cayan, 1996; McCabe and Dettinger, 2002). Oscillating at different periods, ENSO changes phase every 1-3 years whereas the PDO changes every 20-30 years. As a result, the potential representation of each in the mass balance record will be different. With the PDO, we looked for the potential impact in long term balance means. On the other hand, the short-term fluctuations associated with ENSO might be manifested in annual balances. Therefore, we calculate the correlation coefficient *r* relating the ENSO index to net balance and its components over the entire record as well as specific time periods. Because correlations are strongest when comparing climate patterns with the ENSO index a few months prior (Redmond and Koch, 1991), we compare the September-October (S-O) MEI with winter balance and the December-January (D-J) MEI with summer balance. Net balance is related to both. Testing the statistical significance of *r* allows us to differentiate between very strong correlations and those that are insignificant. If correlations are statistically insignificant, we cannot reject our null hypothesis that the slope of the regression line produced between ENSO index and balance is different than zero, indicating no linkage exists between ENSO and glacier mass balance.

By calculating the correlation coefficient between each balance component (i.e., b_w and b_s), we might be able to infer the mechanism by which ENSO and glacier balance are connected if a significant relationship exists. In Table 3.6, we see that for the entire period of record for each glacier, a strong correlation exists between the MEI and winter balance. The strength of the relationship also consistently increases moving north, from an *r* of -0.36 with Jefferson Park to -0.48 with South Cascade. On the other hand, only South Cascade summer balance has a weak correlation with the MEI from 1950-2006. No relationship exists for the remaining southern glaciers. Merely based on these results, we might propose that the strength of the correlation between balance components and ENSO weakens moving south from a high at South Cascade to a low at Jefferson Park. However, strong winter balance correlations exist for each glacier. The ENSO link to summer balance is weak, and there is only a feeble correlation at South Cascade that is nonexistent when looking at the other glaciers to the south.

Table 3.6: Balance component correlations (*r*) with MEI Index

Glacier	b_s - MEI (D-J)			b_w - MEI (S-O)		
	50-85	**86-06**	**All**	**51-85**	**86-06**	**All**
SC	0.06	-0.71***	-0.23*	-0.54***	-0.39*	-0.48***
T	0.09	-0.65***	-0.15	-0.50***	-0.37	-0.46***
WR	0.09	-0.54***	-0.14	-0.39**	-0.28	-0.36***
JP	0.28	-0.42*	-0.04	-0.43**	-0.32	-0.36***

Note: Correlations across the entire period of record and two temporal subsets are displayed. Triple asterisk (***), double asterisk (**), and asterisk (*) represent >99%, >95%, and >90% confidence respectively.

Breaking the time series into two periods exposes an interesting pattern between ENSO and mass balance components. The MEI correlation with winter balance is strengthened for each glacier from 1951-85 and weakened from 1986-2006. From Table 3.6, we conclude that although winter balance is strongly correlated with ENSO from 1951-2006, the relationship has weakened in recent years. In contrast, summer balance exhibits absolutely no correlation with ENSO from 1950 to 1985. After 1985, strong correlations emerge for South Cascade (*r* = -0.71), Tahoma (*r* = -0.65), and White River (*r* = -0.54) glaciers. Jefferson Park (*r* = -0.42) shows a slightly weaker yet still

significant correlation. Again, a north-south trend in strength is apparent. Curiously, in the mid-80s ENSO correlation with summer balance was suddenly "turned on" for all glaciers, once again stressing the importance of temporal variation in correlation.

Correlations between net balance and both the S-O and D-J MEI indices produce nearly identical results. Table 3.7 shows that only a weak correlation exists between net balance and South Cascade glacier between 1950 and 1985, but from 1986-2006, significant correlations exist, some very strong, for all the glaciers. When the entire period is considered, negative trends are apparent for all glaciers, weakening in significance in the observed north-south trend. All correlations were tested through replication using the Southern Oscillation Index (SOI).

Table 3.7: Net balance correlations (*r*) with MEI Index

Glacier	b_n - MEI (D-J)			b_n - MEI (S-O)		
	50-85	86-06	All	51-85	86-06	All
SC	-0.31*	-0.60***	-0.44***	-0.35**	-0.58***	-0.45***
T	-0.10	-0.67***	-0.31**	-0.20	-0.61***	-0.35***
WR	-0.10	-0.56***	-0.30**	-0.16	-0.50**	-0.31**
JP	-0.02	-0.51**	-0.25*	-0.10	-0.47**	-0.28**

Note: Correlations across the entire period of record and two temporal subsets are displayed. Triple asterisk (***), double asterisk (**), and asterisk (*) represent >99%, >95%, and >90% confidence respectively.

Putting these results together, a complicated relationship between balance components and ENSO is exposed. Winter balance has witnessed a recent weakening of its correlation with ENSO, but overall there is a significant inverse relationship. Summer balance, however, did not vary with ENSO until the mid-1980s when a significant positive correlation between the two appears. Only South Cascade net balance shows a weak correlation with ENSO between 1950 and 1985, yielding an interesting result considering the magnitude of winter balance correlations with ENSO. We infer that South Cascade net balance is more sensitive to changes in the winter balance than the southern glaciers. From 1986-2006, summer balance dominates the correlation between net balance and ENSO, highlighting the extreme influence of summer ablation on the net balance for all of the glaciers. To summarize, the glaciers have typically received more

(less) accumulation during La Niña (El Niño) events over the past 50+ years. Only since 1985 has a pattern of less (more) ablation during La Niña (El Niño) events emerged.

The cause of this change in correlation between the balance components in the mid-1980s is currently unknown and beyond the scope of this study. However, a few hypotheses are presented:

(1) *Model results are erroneous and the strong correlations with summer balance between 1985 and 2006 are not real.* However attractive this conclusion initially seems, producing erroneous results that correlate with the ENSO index for *all* of the glaciers would be nearly impossible. Since each of the four study glaciers are individually optimized, the replication of this correlation indicates that it is most likely real. Furthermore, when correlating USGS *in situ* measurements at South Cascade glacier with the ENSO index, the same pattern is attained. No correlation exists between the D-J MEI index and summer balance between 1959 and 1985. From 1986 to 2004, a significant correlation coefficient of -0.78 ($p < 0.001$) appears, which is extremely similar to the correlation of -0.71 ($p < 0.001$) with modeled results. Therefore, the mid-80s shift in correlation between the summer balance and ENSO is real.

(2) *The effects of El Niño have been amplified since the 1976/77 shift back into a warm PDO phase, leading to enhanced melt effects.* Gershunov and Barnett (1998) empirically determine that PDO phase can modulate teleconnections associated with ENSO. During a warm (cool) PDO phase, the influence of El Niño (La Niña) is heightened in North America. Since El Niño years are typically accompanied by less winter precipitation resulting from warmer temperatures and less precipitation and are becoming more frequent, perhaps a new relationship between melt and ENSO is developing. During 1950-1976, if the impact of La Niña was heightened, a significant relationship between melt and ENSO would not have developed. During a cool PDO phase, typically winter temperatures are depressed and precipitation is enhanced in the PNW. As compared to an ENSO neutral year, melt would not change much during a positive (El Niño) ENSO year because its impacts are reduced. Similarly, during a negative (La Niña) year,

further dampening of the temperature would not have as large of an effect since temperature is already decreased due to the PDO. However, because no correlation between summer balance and ENSO exists for South Cascade and White River glaciers during the early warm period from 1927-1945, we do not believe that El Niño amplification resulting from a warm PDO phase is responsible. Furthermore, we would expect the relationship to develop in the late-70s, coinciding with the PDO phase shift and not in the mid-80s.

(3) *ENSO manifestation in regional climate changed including a stronger link to spring/summer temperatures.* Redmond and Koch (1991) quantified the relationship between ENSO and surface climate for the entire Western United States and discovered no significant correlation existed between ENSO and summer (April – September) temperature and precipitation. However, their study only includes data up to 1984. Beebee and Manga (2004) also correlate climate and ENSO in Oregon, including data up to the late-90s, and find that some of their winter and spring temperature records do weakly correlate with ENSO. Changes in that relationship with time, however, are not considered.

To determine whether the correlation between ENSO and temperature changes in the mid-1980s, we averaged the monthly temperatures for positive and negative index years separately before and after 1985. Using minimum temperature at Longmire as an example, we see in Figure 3.7 that the difference in average temperature increases after 1985 especially in the spring/summer months. We might assume that ENSO fluctuations prior to 1985 did not affect summer ablation nearly as much as after 1985. Investigating further, we compared the correlation coefficients (Table 3.8) before and after 1985 between ENSO and both the minimum and maximum temperature observations at three stations used in this study: Diablo Dam, Longmire, Three Lynx.

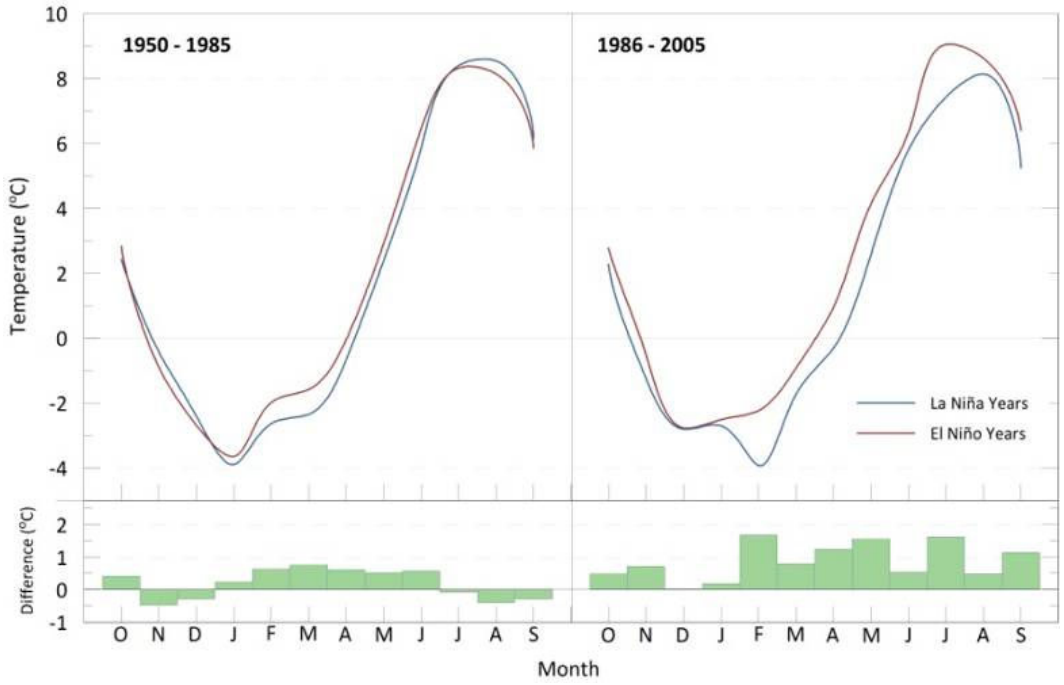

Figure 3.7: Monthly average minimum temperatures at Longmire during El Niño and La Niña years for 1950-1985 and 1986-2005. The difference in monthly average between the two phases is shown below for each of the two periods. Spring/Summer temperatures differences are much larger between 1986 and 2005 than previously.

Table 3.8: Correlations (*r*) relating temperature and MEI (D-J)

Station	T_{min}		T_{max}	
	50 - 85	**86 - 05**	**50 - 85**	**86 - 05**
Diablo Dam	0.39**	0.66***	0.18	0.60***
Longmire	0.29*	0.57***	0.07	0.45**
Three Lynx	0.20	0.41*	0.12	0.30

N ↑

Note: Stations are listed relative to north. Correlations from two temporal subsets are displayed. Triple asterisk (***), double asterisk (**), and asterisk (*) represent >99%, >95%, and >90% confidence respectively.

Our results presented in Table 3.8 indicate that after 1985 the correlation between April-August average temperature and ENSO has become much stronger for both minimum and maximum observations. The strongest (weakest) relationship occurs at the northern(southern)most station. We conclude that ablation, once weakly related to ENSO fluctuations, is now strongly linked to

ENSO through spring/summer temperature. Therefore, ENSO influence on PNW climate was possibly modified in the mid-1980s leading to a stronger link between the ENSO index and spring/summer temperature and ultimately glacier ablation. We also surmise that due to the ice-albedo feedback, the ENSO relationship with ablation is higher than temperature observations.

Based on these findings, we conclude that the correlation between ENSO and glacier mass balance exhibits strengthening since the mid-1980s due to temperature fluctuations that coincide with ENSO variations. Since 1985, El Niño years are accompanied by high glacier ablation and *vice versa*. Winter balance has remained linked to ENSO throughout the entire period; however, a weakening might be occurring. Because of the large influence of melt on these glaciers, only since 1985 has net balance been correlated with ENSO with the exception of South Cascade glacier. The northward strengthening of these correlations is most likely the cause.

3.10 Climate Sensitivity Analysis

To determine the potential response of glacier mass balance to multiple climate change scenarios, we calculated the change in the mean net mass balance from 1977-2003 resulting from each perturbation. Although climate change involves the complex interaction of many climatic variables (e.g., temperature, precipitation, humidity, wind speed, cloudiness), we are limited by model inputs and only assess temperature and precipitation variation.

Balance sensitivity estimates using six temperature and four precipitation perturbations are displayed in Figure 3.8 for each glacier. South Cascade glacier is the least responsive to temperature fluctuations with a sensitivity of -0.73 mw.e. $°C^{-1}$ (assuming a linear relationship between temperature and mass balance changes). This estimate for South Cascade glacier is in near perfect agreement with Rasmussen and Conway's (2003) -0.75 mw.e. $°C^{-1}$ calculation. Tahoma and White River have nearly equal sensitivities of -0.99 and -0.98 mw.e. $°C^{-1}$ respectively, and Jefferson Park is the most responsive at -1.09 mw.e. $°C^{-1}$. Even though the temperature sensitivity was assumed linear for simplicity, we observe in Figure 3.8 that the relationship is in fact

non-linear. That is not the case for the precipitation sensitivity. South Cascade and Jefferson Park are the most susceptible to changes in precipitation as their sensitivities are +0.26 and +0.25 mw.e. $(+10\%)^{-1}$, followed by Tahoma and White River glaciers at +0.23 and +0.17 mw.e. $(+10\%)^{-1}$ respectively. These values suggest that a 1°C temperature increase could potentially be balanced by a synchronous 30% increase in winter precipitation at South Cascade glacier. For the remaining glaciers, >40% increase in winter precipitation is necessary to offset the 1°C temperature increase.

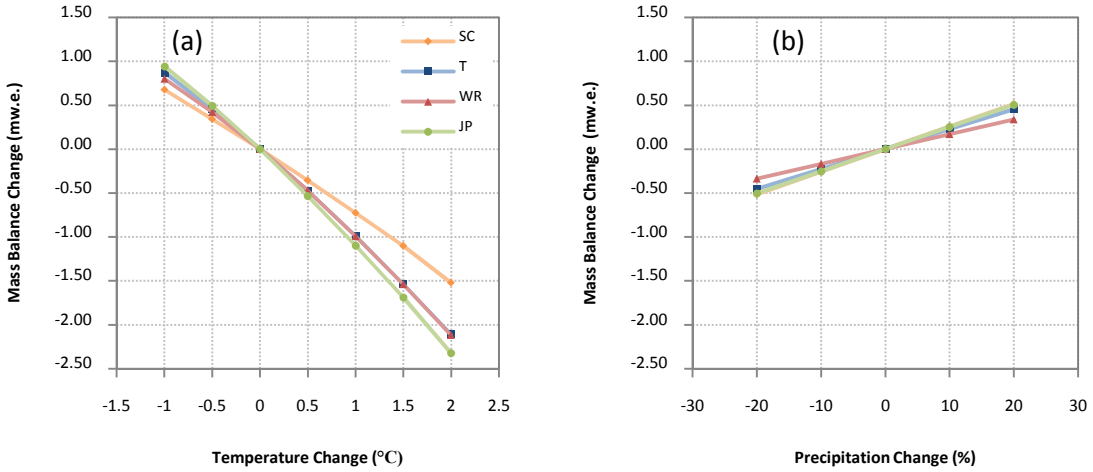

Figure 3.8: Net balance sensitivity calculations for changes in (a) temperature and (b) precipitation for each study glacier. While all the glaciers have similar precipitation sensitivities, the temperature sensitivity of South Cascade stands out, much lower than the other glaciers.

South Cascade additionally differs from the other glaciers since temperature significantly influences both the winter and summer balance components. For a temperature rise of 1°C at South Cascade, the winter and summer balances decrease 0.12 and 0.61 mw.e. respectively, combining to a net balance decrease of 0.73 mw.e. Although temperature dominates the summer balance, the change in winter balance accounts for just over 15% of the change in net balance. Only 5% of the change in net balance results from the change in the winter balance for the remaining glaciers.

Our ability to assess regional sensitivity patterns is hindered by our sample size. The addition of a few more glacier sensitivity estimates would provide us with a more confident understanding of glacier climate sensitivity in the PNW. Because the study

glaciers exist across a large North-South gradient, we assume that the influence of such a gradient will dominate temperature sensitivities and any effect of glacier hypsometry would be overpowered. This dependence is visible in temperature sensitivity results which decrease as latitude increases. A sensitivity study conducted for glaciers on Mount Hood, for example, could emphasize differences resulting from different glacier geometries. No clear patterns were observed for precipitation sensitivity estimates.

3.11 Future Glacier Extent

We used model results from different temperature scenarios to estimate new equilibrium glacier size (Table 3.9). Not surprisingly, the southernmost glaciers are the most sensitive to temperature change even though they occupy higher elevations on average. However, geometry changes cannot simply be inferred from mass balance; they are tightly linked to balance and the area altitude distribution of the glacier. Glacier changes were determined by modeling the current glacier under a given climate scenario and subsequently removing altitude bands beginning at the terminus until the glacier reaches equilibrium. Therefore, this new glacier represents the possible equilibrium extent of the glacier in a *constant* climate with the same balance dynamics currently in control. Because glacier length responds slowly and climate is constantly changing, these equilibrium glaciers only help us to visualize the effects of different climate scenarios and are not necessarily representative of actual changes. Furthermore, the glacier will also be subject to local balance effects (e.g., topographic shading, aspect, slope).

South Cascade glacier would undergo the most dramatic change in size in a warming climate, a product of its current state of disequilibrium as well as its low average elevation. White River and Jefferson Park glaciers are essentially in equilibrium with the current climate, whereas South Cascade and Tahoma glaciers are not as their average net balance between 1977 and 2006 are both negative. This divergence is most likely a result of longer response times for South Cascade and Tahoma due to small slope and extreme length respectively. Without changing climate, South Cascade must shed 23% of its area and retreat ~150 vertical meters to reach equilibrium (Figure 3.9). We will base our estimates of glacier change on the glacier equilibrium extent under the current climate.

Table 3.9: Glacier geometry changes under two warming scenarios

Glacier	Terminus (masl)				Area (km^2)			
	Current	Eq.[a]	+ 1° C	+ 2° C	Current	Eq.[a]	+ 1° C	+ 2° C
SC	1635	1800	1920 (+120 m)	DNE[b]	1.88	1.45	0.66 (-55%)	0.00 (-100%)
T	1845	2030	2325 (+295 m)	2525 (+495 m)	6.39	5.94	5.05 (-15%)	4.05 (-30%)
WR	2210	2210	2310 (+100 m)	2510 (+300 m)	0.38	0.38	0.30 (-20%)	0.23 (-40%)
JP	2215	2215	2435 (+220 m)	2635 (+420 m)	0.50	0.50	0.28 (-45%)	0.10 (-80%)

[a] Terminus or area associated with the glacier in equilibrium with the current climate. Applies to SC and T only.

[b] Does not exist. Glacier has been annihilated.

Note: Changes in glacier terminus elevation and area under two warming scenarios. Percentages are relative to the equilibrium glacier in order to faciliate comparison between glaciers.

Values of terminus altitude and area change for both a 1 and 2°C temperature increase are shown. Figures 3.9-3.12 show hypothesized changes in glacier geometry under the different warming scenarios. A 2°C warming is enough to eliminate South Cascade glacier. However, even in this warm climate, Tahoma, White River, and Jefferson Park could potentially exist, albeit much smaller in size. These results are just as expected. Glaciers that extend into high elevations will still exist in conditions conducive to glacier activity. South Cascade reaches maximum elevation at 2110 m, below the current equilibrium terminus of two of the other glaciers. Furthermore, percent area loss increases with decreasing maximum elevation as the glacier cannot offset negative balances in the low elevation area. Our results draw out the weakness in glacier static climate sensitivity: glacier modification is not incorporated. The retreat of South Cascade glacier will not affect its temperature sensitivity because it exists across a small elevation range. However, changing the geometry of the remaining glaciers will have a dramatic effect on their sensitivity since they cover a larger elevation range. Consequently, low maximum elevation glaciers will be most dramatically shaped by a warming climate even in the northern part of the region. The glaciers on the Cascade strato-volcanoes could potentially persist even after a warming of 2°C, retreating towards their lofty summits (Figures 3.10-3.12). Those at low elevations could retreat into zones of topographic shading, but those on exposed southern faces might not be as fortunate.

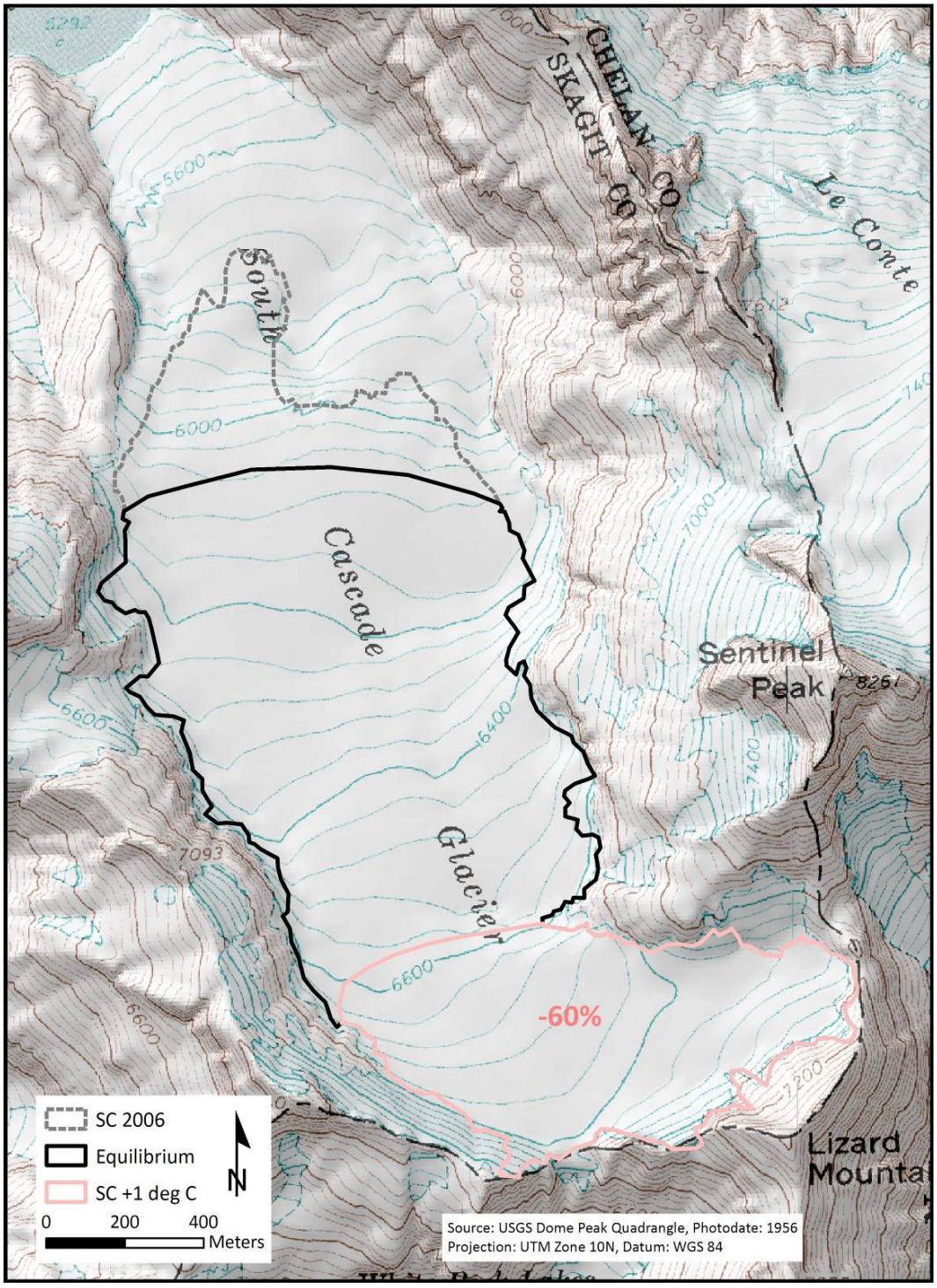

Figure 3.9: South Cascade glacier topography with current glacier extent, hypothesized equilibrium glacier and glacier under a 1° C warming. Note there is not a glacier extent for a warming of 2°C because the glacier would simply not exist without local topographic effects. The glacier under a 1°C rise in temperature would be 60% smaller than the equilibrium glacier.

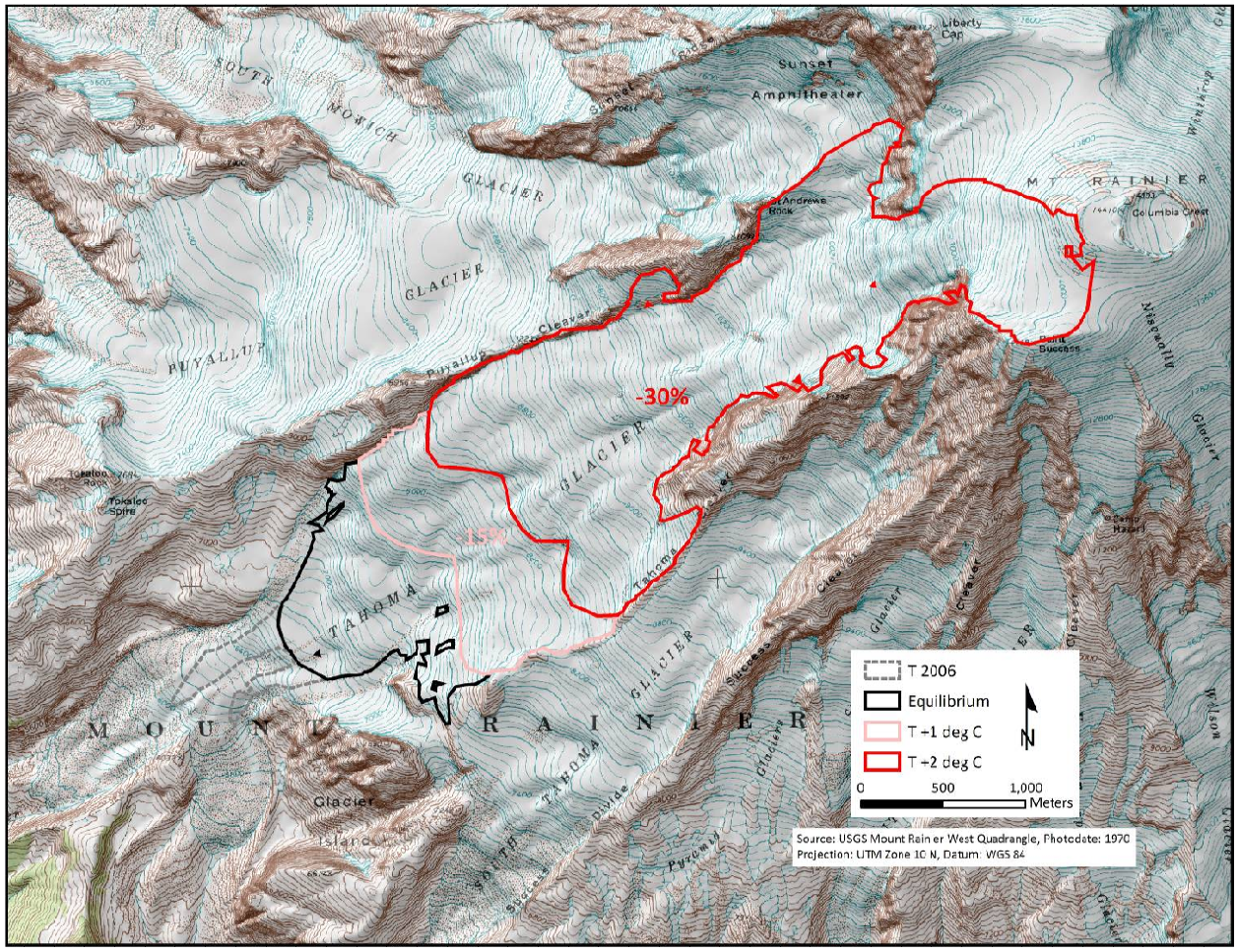

Figure 4.10: Tahoma glacier topography with current glacier extent, hypothesized equilibrium glacier and glaciers under 1 and 2° C warming scenarios. The glacier under 1 and 2°C rises in temperature would be 15% and 30% smaller respectively than the equilibrium glacier. Local affects are not considered; the glacier is assumed to retreat starting at the terminus moving upward.

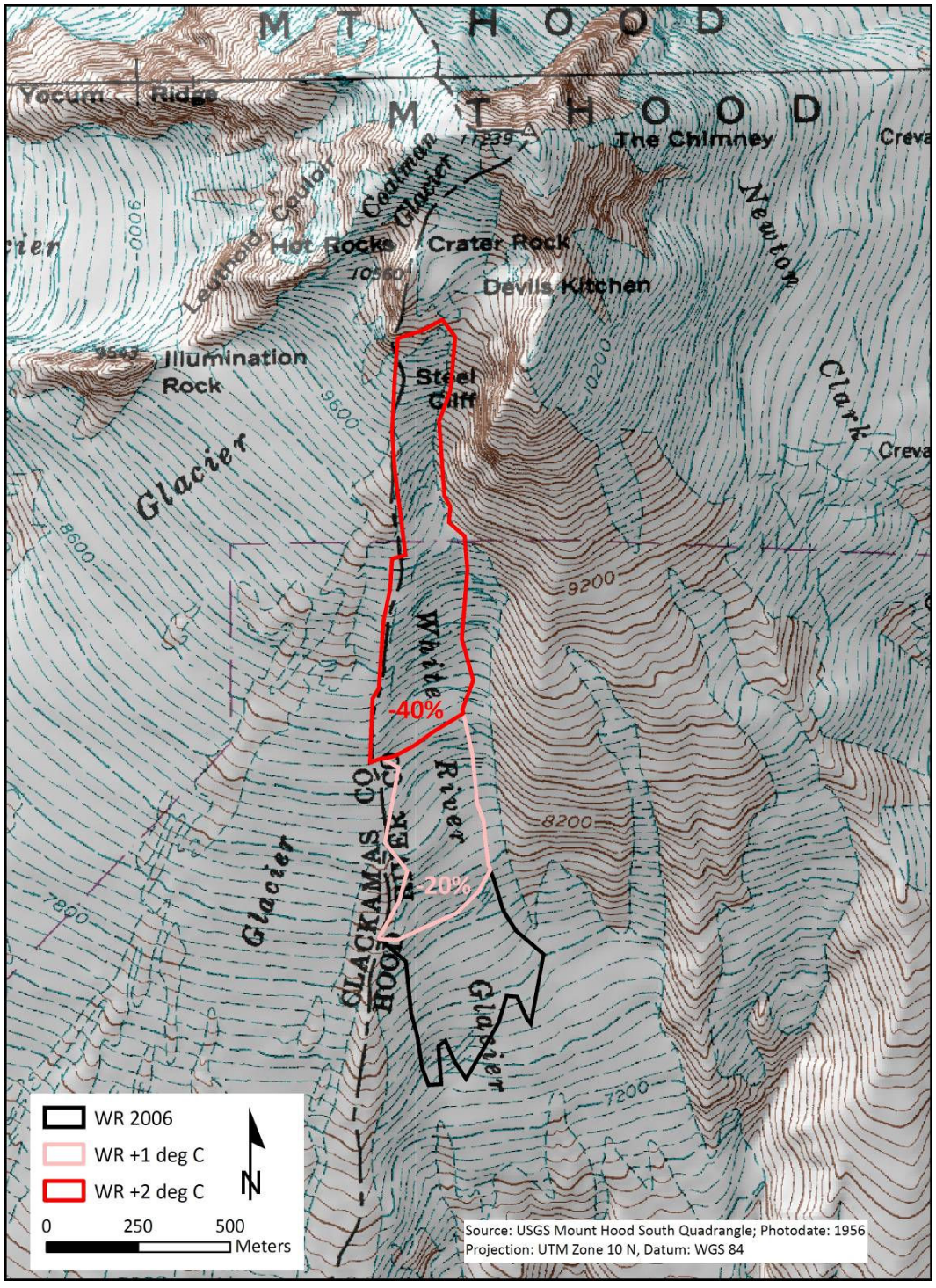

Figure 3.11: White River glacier topography with current glacier extent and glaciers under 1 and 2° C warming scenarios. The glacier under 1 and 2°C rises in temperature would be 20% and 40% smaller respectively than the current glacier. Local affects are not considered; the glacier is assumed to retreat starting at the terminus moving upward.

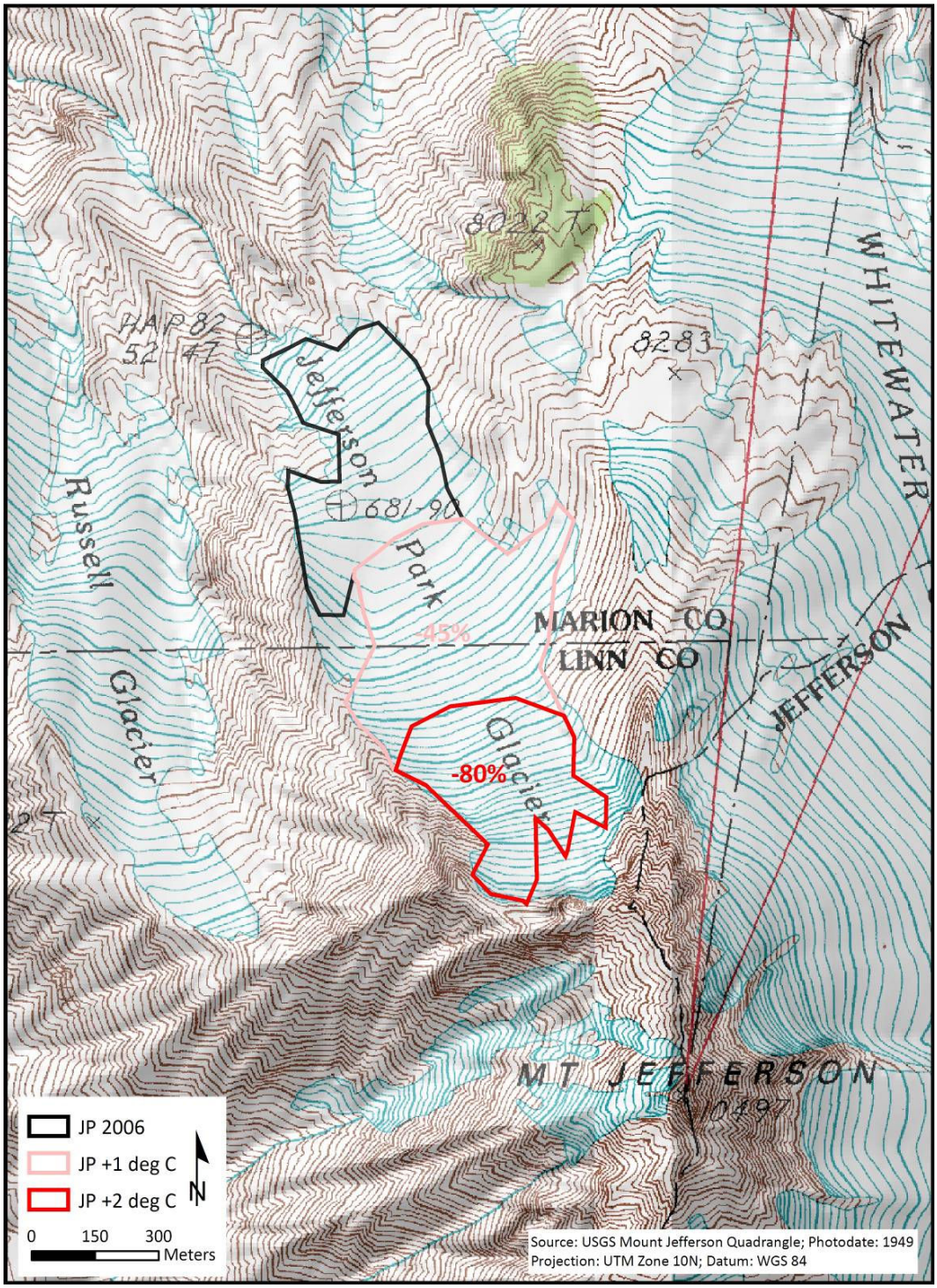

Figure 3.12: Jefferson Park glacier topography with current glacier extent and glaciers under 1 and 2° C warming scenarios. The glacier under 1 and 2°C rises in temperature would be 45% and 80% smaller respectively than the equilibrium glacier. Local affects are not considered; the glacier is assumed to retreat starting at the terminus moving upward.

3.12 Conclusions

The relationship between climate fluctuations and glacier mass balance were investigated through comparison with the PDO and ENSO and calculation of balance sensitivity to multiple climate perturbations using a simple mass balance model. Our results indicate that balance correlation with ENSO has become more significant than PDO in the recent past. The 1945/46 PDO phase shift is apparent in our model results, but the 1976/77 is ambiguous, only weakly visible for South Cascade glacier. Therefore, a future transition into a PDO cool phase might only shift South Cascade into a period of slightly less melt and more accumulation. The lack of balance results from more than two phase shifts in combination with recent trend weakening leaves us unconvinced that the relationship is real. However, the nascent and unmistakable strengthening of the correlation between ENSO and balance (more specifically, summer balance) might be overpowering the PDO signal.

Prior to the mid-1980s, ENSO was negatively correlated with winter balance only but not enough to significantly influence net balance. Afterwards, a strong negative relationship with summer balance in addition to winter balance resulted in significant correlations between ENSO and net balance. Accordingly, we infer that the summer balance is a more important component than winter balance in determining the net balance for these glaciers. The extreme shift in the influence of the oscillation on summer balance relates to a strengthening of the relationship between ENSO and spring/summer temperature, especially daily minimums, during the 1980s. It is also important to note that the strength of the ENSO correlations increase with latitude. Since these correlation coefficients exceed those related to the PDO, we expect ENSO fluctuations to subdue the influence of the PDO. A better understanding of this link in addition to the potential modulation due the PDO could aid in short term prediction of glacier mass balance based partly on ENSO phase.

Climate sensitivity estimates did not expose potential hypsometric influences due to the overpowering impact of latitude. The decrease in temperature sensitivity with increasing latitude is most likely a product of reduced incoming solar radiation and lower

temperatures. However, no pattern in precipitation was discernable with similar results for all the glaciers. Thus, a large gradient in balance sensitivity exists. The northernmost glacier, South Cascade, could offset a 1°C rise in air temperature by a 30% increase in winter precipitation, but the southernmost glacier, Jefferson Park, requires >40% increase to compensate. These sensitivities give us a baseline for potential impacts of climate change, but glacier hypsometry also plays a role in the future health of each glacier.

To aid in the interpretation of the climate sensitivity estimates, we made simple estimations of future glacier geometry based on two warming scenarios. In the absence of the influence of aspect and topographic shading, South Cascade glacier would be in complete disequilibrium and could not exist under a 2°C warming. For the high altitude glaciers, equilibrium is reached through significant retreat uphill, especially for the southern glaciers. Based on these responses, we infer that South Cascade glacier temperature sensitivity, unlike the sensitivities of the remaining glaciers, does not change rapidly enough as the glacier retreats to reach a new equilibrium under the temperature increase. In a sense, the low slope, low altitude South Cascade does not "look" extremely different as it retreats, whereas the remaining steeply-sloped glaciers do as they incorporate a large range in elevation. With time, all the glaciers can reach an equilibrium state with a 1°C temperature increase. However, South Cascade cannot exist under a 2°C warming since retreat was not capable of decreasing its sensitivity. These results underscore the importance of the area altitude distribution of a glacier when making a future diagnosis of health and persistence. The simple calculations of change in glacier size helped us to make fair interpretations of glacier sensitivity. Even though South Cascade is the least sensitive to temperature change currently, it will ultimately be affected the most dramatically due to its low elevation.

Many of the change scenarios used are good estimates of future regional climate change. Results from the IPCC Report (Christensen *et* al., 2007) show that the Pacific Northwest can expect annual temperatures to rise by approximately 3°C and winter precipitation to increase about 10% by 2080-2099. Therefore, it is likely that our maximum temperature scenario of +2°C will be reached within the next century.

However, a 10% rise in winter precipitation cannot even counteract an annual temperature rise of 0.5° C at any of the glaciers, dampening a 2° C temperature rise slightly. Even though the lagged response time of a glacier will extend the life of the glacier, without a future cooling or unexpected jump in winter precipitation, many of the glaciers especially at the lowest elevations may simply disappear.

Chapter 4 – Conclusion

Although the methodologies presented in each paper can be used independently to monitor glacier health, a more complete glacier assessment is obtained when they are used in conjunction. Results from the first paper provide an updated glacier inventory that acts as a baseline for observing future glacier change on the landscape. However, climate-glacier interactions cannot be investigated. Results from the second paper address such issues, but without an updated glacier inventory, the vulnerability of *current* glaciers could not be determined. Furthermore, climate impact results from the second paper can be extrapolated throughout the region based on glacier distribution characteristics estimated in the first paper, providing a better regional view of glacier health.

Based on the satellite derived glacier inventory, over 230 km^2 of glacier features were mapped in the North Cascades National Park, Olympic Mountains, and Cascade Volcanoes for 2002-2006. The largest deviations (-30%) from the USGS baseline occur in the Cascade Volcanoes followed by the North Cascades (-16%). Current glacier cover in the Olympics is essentially the same as its 1987 USGS baseline. However, comparison between these three sub-regions to investigate climate controls on glacier size is futile as the baseline date is inconsistent. Therefore, we use updated glacier boundaries in a simple mass balance model for four glaciers in the Pacific Northwest to more accurately investigate the interaction between climate and glacier health.

To realistically estimate the current potential impact of climate change on glacier health using a mass balance model, recent glacier hypsometric characteristics are needed. Using glacier geometry from USGS topographic maps would have provided an outdated look at climate dynamics. Therefore, it is imperative that current area altitude profiles are used. Our temperature sensitivity results range from -0.73 to -1.09 mw.e. $°C^{-1}$; however, South Cascade glacier is the least sensitive to temperature yet will experience the largest retreat in a warming climate. Such interesting results underscore the importance of using an updated area altitude distribution when making a future diagnosis of glacier health.

Using results from both papers provides a more comprehensive picture of the potential impact of climate change on glaciers in the Pacific Northwest. Since mass balance was not modeled for an Olympic glacier, we are not able to confidently ascribe estimates of future change. However, because these glaciers have seen relatively little change in area since 1987, we can clearly separate them from glaciers elsewhere in the Pacific Northwest. As the glaciers of the North Cascades inhabit elevations between 1085 and 2720 m, we consider them the most at risk and will experience the largest loss in ice cover. Glaciers of the Cascade Volcanoes occupy very low and high elevations (1405 – 4395 m) and are capable of retreating to an elevation that is high enough to escape the impact of a warming climate. Therefore, glaciers that extend to low elevations can potentially be sustained by accumulation at high elevations whereas glaciers without a high altitude accumulation area will be severely reduced in size. As a result, the higher latitude glaciers of the North Cascades Park are at a much higher risk for extinction than the lower latitude glaciers of the Cascade Volcanoes. That is not to say that the glaciers of the Cascade Volcanoes will be unaffected; instead, these glaciers will persist on the landscape longer in a warming climate. These results confirm the presence of three distinct zones of glaciation in the Pacific Northwest, indicating monitoring a single benchmark glacier cannot capture the entire regional picture of glacier dynamics.

The papers presented provide a capable method for remotely monitoring glacier health and dynamics. Carefully selected satellite imagery can provide an updated glacier inventory that not only provides a baseline for comparison but also current glacier characteristics that fuel a simple mass balance model. The model presented is unique as it can be applied to any glacier throughout the globe that is within 50 km of a meteorological station. Therefore, the potential impact of climate change can be investigated for glaciers that are too dangerous or remote by incorporating the outlined method. Combining the two procedures makes investigating comprehensive regional glacier characteristics possible.

BIBLIOGRAPHY

An, S. and B. Wang, 2000: Interdecadal change of the structure of the ENSO mode and its impact on the ENSO frequency, 13, 12: 2044-2055.

Arnold, N.S., I.C. Willis, M.J. Sharp, K.S Richards, and W.J. Lawson, 1996: A distributed surface energy-balance model for a small valley glacier. I. Development and testing for Haut Glacier d'Arolla, Valais, Switzerland. *Journal of Glaciology*, 42, 140: 77-89.

Albert, T.H., 2002: Evaluation of remote sensing techniques for ice-area classification applied to the tropical Quelccaya ice cap, Peru. *Polar Geography*. 26: 210-226.

Barnett, T.P., J.C. Adam, D.P. Lettenmaier, 2006: Potential impacts of a warming climate on water availability in snow-dominated regions. *Nature*, 438: 303-309.

Barton, R. R. and J. S. Ivey, 1996: Nelder-Mead Simplex Modifications for Simulation-Optimization. *Management Science*, 42: 954-973.

Barry, R.G., 2006: The status of research on glaciers and global glacier recession: a review. *Progress in Physical Geography*, 30, 3: 285-306.

Beebee, R.A. and M. Manga, 2004: Variation in the relationship between snowmelt runoff in Oregon and ENSO and PDO. *Journal of the American Water Resources Association*, 40, 4: 1011-1024.

Benn, D.I. and D.J.A. Evans, 1998: Glaciers and Glaciation. Oxford University Press, New York, NY: 734pp.

Bhatt, U.S., J. Zhang, C.S. Lingle, L.M. Phillips, and W.V. Tangborn, 2007: Examining glacier mass balances with a hierarchical modeling approach. *Computing in Science and Engineering*, 9, 2: 60-67.

Bidlake, W.R., E.G. Josberger, and M.E. Savoca, 2005: Water, ice, and meteorological measurements at South Cascade Glacier, Washington, balance year 2003: U.S. Geological Survey Scientific Investigations Report 2005-5210: 48pp.

Bidlake, W.R., E.G. Josberger, and M.E. Savoca, 2007: Water, ice, and meteorological measurements at South Cascade Glacier, Washington, balance years 2004 and 2005. U.S. Geological Survey Scientific Investigations Report 2007-5055: 70pp.

Braithwaite, R.J. and O.B. Oleson, 1989: Calculation of glacier ablation from air temperature, West Greenland. In: *Glacier Fluctuations and Climatic Change* [Oerlemans, J. (ed.)]. Kluwer Academic Publishers, Dordrecht, Netherlands: pp.219-233.

Braithwaite, R.J. and Y. Zhang, 1999: Modelling changes in glacier mass balance that may occur as a result of climate changes. *Geografiska Annaler*, 81A, 4: 489-496.

Brock, B.W., I.C. Willis, and M.J.Sharp, 2000: Measurement and parameterization of albedo variations at Haut Glacier d'Arolla, Switzerland. *Journal of Glaciology*, 155: 675-688.

Cayan, D.R., 1996: Interannual climate variability and snowpack in the Western United States, *Journal of Climate*, 9, 5: 928-948.

Chavez, P.S., Jr., 1975: Atmospheric, solar, and MTF corrections for ERTS digital imagery. *Proceedings of the American Society of Photogrammetry*, Fall Technical Meeting, Pheonix, AZ, p69.

Chennault, J.W., 2004: Modeling the contributions of glacial meltwater to streamflow in Thunder Creek, North Cascades National Park, Washington. Unpublished Thesis (M.S.), Western Washington University, 78pp.

Chiarle, M., S. Iannotti, G. Mortara, and P. Deline, 2007: Recent debris flow occurrences associated with glaciers in the Alps. *Global and Planetary Change,* 56: 123-136.

Christensen, J.H., B. Hewitson, A. Busuioc, A. Chen, X. Gao, I. Held, R. Jones, R.K. Kolli, W.-T. Kwon, R. Laprise, V. Magaña Rueda, L. Mearns, C.G. Menéndez, J. Räisänen, A. Rinke, A. Sarr and P. Whetton, 2007: Regional Climate Projections. In: *Climate Change 2007: The Physical Science Basis. Contribution of Working Group I to the Fourth Assessment Report of the Intergovernmental Panel on Climate Change* [Solomon, S., D. Qin, M. Manning, Z. Chen, M. Marquis, K.B. Averyt, M. Tignor and H.L. Miller (eds.)]. Cambridge University Press, Cambridge, United Kingdom and New York, NY, USA.

Clark, M. P., M. C. Serreze, and G. J. McCabe, 2001: The historical effect of El Niño and La Niña events on the seasonal evolution of the montane snowpack in the Columbia and Colorado River basins. *Water Resources Research,* 37: 741-757.

Dozier, J., 1989: Spectral signature of alpine snow cover from the Landsat Thematic Mapper. *Remote Sensing of the Environment*, 28: 9-22.

Driedger, C.L. and P.M. Kennard, 1986: Ice volumes on Cascade volcanoes: Mount Rainier, Mount Hood, Three Sisters, and Mount Shasta, U.S. Geological Survey Professional Paper 1365: 28pp.

Dyurgerov, M .B. and M. F. Meier, 1997: Year-to-year fluctuation of global mass balance of small glaciers and their contribution to sea level changes. *Arctic and Alpine Research*, 29, 4: 392-401.

---, 2005: Glaciers and the changing Earth system: A 2004 snapshot. Institute of Arctic and Alpine Research, University of Colorado, Boulder, Colorado, Occasional Paper, 58: 117pp.

Furbish, D.J. and J.T. Andrews, 1984: The use of hypsometry to indicate long-term stability and response of valley glaciers to changes in mass transfer, *Journal of Glaciology*, 30, 105: 199-211.

Granshaw, F.D., 2002: Glacier change in the North Cascades National Park Complex, Washington State USA, 1958 to 1998. Unpublished Thesis (M.S.), Portland State University: 134pp.

Granshaw, F.D. and A.G. Fountain, 2006: Glacier change (1958-1998) in the North Cascades National Park Complex, Washington, USA. *Journal of Glaciology*, 52, 177: 251-256.

Gershunov A. and T. Barnett, 1998: Interdecadal modulation of ENSO teleconnections. *Bulletin of the American Meteorological Society*, 79: 2715-2726.

Heliker, C.C., A. Johnson, and S.M. Hodge, 1984: The Nisqually Glacier, Mount Rainier, Washington, 1857–1979: A summary of the long-term observations and a comprehensive bibliography. U.S. Geological Survey Open-File Report 83-541: 20pp.

Hock, R., 2003: Temperature index melt modelling in mountain areas. *Journal of Hydrology*, 282: 104-115.

Howat, I.M., S. Tulaczyk, P. Rhodes, K. Israel, and M. Snyder, 2007: A precipitation-dominated, mid-latitude glacier system: Mount Shasta, California. *Climate Dynamics*, 28, 1: 85-98.

Josberger, E.G., W.R. Bidlake, R.S. March, and B.W. Kennedy, 2007: Glacier mass-balance fluctuations in the Pacific Northwest and Alaska, USA. *Annals of Glaciology*, 46: 291-296.

Klok, E.J. and J. Oerlemans, 2004: Modelled climate sensitivity of the mass balance of Morteratschgletscher and its dependence of albedo parameterization. *International Journal of Climatology*, 24: 231-245.

Krimmel, R.M., 1989: Mass balance and volume of South Cascade Glacier, Washington, 1958–1985. In: *Glacier fluctuations and climatic change* [Oerlemans, J. (ed.)]. Kluwer Academic Publishers, Dordrecht, Netherlands: pp.193-206.

---, 1999: Analysis of difference between direct and geodetic mass balance measurements at South Cascade glacier, Washington. *Geografiska Annaler*, 81A, 4: 653-658.

Lauman, T. and N. Reeh, 1993: Sensitivity to climate change of the mass balance of glaciers in southern Norway. *Journal of Glaciology*, 39, 133: 656-665.

Lemke, P., J. Ren, R.B. Alley, I. Allison, J. Carrasco, G. Flato, Y. Fujii, G. Kaser, P. Mote, R.H. Thomas, and T. Zhang, 2007: Observations: Changes in snow, ice and frozen ground. In: *Climate Change 2007: The Physical Science Basis. Contribution of Working Group I to the Fourth Assessment Report of the Intergovernmental Panel on Climate Change* [Solomon, S., D. Qin, M. Manning, Z. Chen, M. Marquis, K.B. Averyt, M. Tignor, and H.L. Miller (eds.)]. Cambridge University Press, New York, NY.

Letreguilly, A. and L. Reynaud, 1989: Spatial patterns of mass-balance fluctuations of North American glaciers. *Journal of Glaciology*, 35, 120: 163-168.

---, 1990: Space and time distribution of glacier mass-balance in the Northern Hemisphere. *Arctic and Alpine Research*, 22, 1: 43-50.

Lillquist, K.D., and K. Walker, 2006: Historical glacier and ornate fluctuations at Mt. Hood, Oregon. *Arctic Antarctic and Alpine Research*, 38: 399-412.

Mantua, N.J., 2008 (ongoing updates): PDO index. *Available at* http://jisao.washington.edu/pdo/PDO.latest. *Accessed* January, 2008.

Mantua, N. J., S. R. Hare, Y. Zhang, J. M. Wallace, and R. C. Francis, 1997: A Pacific interdecadal climate oscillation with impacts on salmon production. *Bulletin of the American Meteorological Society,* 78: 1069-1079.

Mantua, N.J. and S.R. Hare, 2002: The Pacific Decadal Oscillation, *Journal of Oceanography*, 58: 35-44.

McCabe, G.J. and M.D. Dettinger, 2002: Primary modes and predictability of year-to-year snowpack variations in the Western United States from teleconnections with the Pacific Ocean climate, *Journal of Hydrometeorology*, 3, 1: 13-25.

Meier, M.F., 1961a: Distribution and variations of glaciers in the United States exclusive of Alaska. In: *General Assembly of Helsinki*, 1960: International Association of Scientific Hydrology Publication, 54: pp.420-429.

---, 1984: Contribution of small glaciers to global sea level. *Science*, 226, 4681: 1418-1421.

Meier, M.F., M.B. Dyurgerov, U.K. Rick, S. O'Neel, W. Tad Pfeffer, R.S. Anderson, S.P. Anderson, and A.F. Glazovsky, 2007: Glaciers dominate eustatic sea-level rise in the 21st Century. *Science*, 317, 5841: 1064-1067.

Miles, E.L., A.K Snover, A.F. Hamlet, B. Callahan, and D. Fluharty, 2000: Pacific Northwest Regional Assessment: The impacts of climate variability and climate change on the water resources of the Columbia River basin. *Journal of the American Water Resources Association*, 36, 2: 399-420.

Mote, P.W., 2006: Climate-driven variability and trends in mountain snowpack in western North America. *Journal of Climate*, **19**: 6209-6220.

NCDC (National Climate Data Center), 2007: Climate data online. National Oceanic and Atmospheric Administration, National Environmental, Satellite, Data, and Information Services (NESDIS). *Available at* http://www7.ncdc.noaa.gov/CDO/cdo. *Accessed in* February, 2007.

NOAA (National Oceanic and Atmospheric Administration), 2008: Monthly atmospheric and SST indices/Southern Oscillation Index (SOI). National Oceanic and Atmospheric Administration, National Weather Service, National Centers for Environmental Prediction, Climate Prediction Center. *Available at* http://www.cpc.ncep.noaa.gov/data/indices/. *Accessed in* January, 2008.

NOAA, 2008: Multivariate ENSO Index (MEI). National Oceanic and Atmospheric Administration, National Weather Service, National Centers for Environmental Prediction, Climate Prediction Center. *Available at* http://www.cdc.noaa.gov/people/klaus.wolter/MEI/table.html. *Accessed in* January, 2008.

NPS (National Park Service), 2007: NPS Stats. National Park Service Public Use Statistics Office. *Available at* http://www.nature.nps.gov/stats/. *Accessed in* July, 2007.

NPS, 2008: November 2006 flood. National Park Service, Mount Rainier. *Available at* http://www.nps.gov/mora/parknews/november-2006-flood-old-page.htm. *Accessed in* March, 2008.

Ohmura, A., 2001: Physical basis for the temperature-based melt-index method. *Journal of Applied Meteorology*, 40: 753-761.

---, 2004: Cryosphere during the twentieth century. In: *The State of the Planet: Frontiers and Challenges in Geophysics* [Sparks, R.S.J. and C.J. Hawkesworth (eds.)]. Geophysical Monograph 150, American Geophysical Union, Washington, DC: pp. 239-257.

---, 2006: Changes in mountain glacier and ice caps during the 20th century. *Annals of Glaciology*, 43: 361-368.

Paul, F., 2002a: Changes in glacier area in Tyrol, Austria, between 1969 and 1992 derived from Landsat 5 TM and Austrian Glacier Inventory data. *International Journal of Remote Sensing*, 23: 787-797.

Paul, F., 2002b: Combined technologies allow rapid analysis of glacier changes, *Eos Transactions*, AGU, 83, 23: pp.253, 260, 261.

Paul, F., A. Kääb, M. Maisch, T. Kellenberger, and W. Haeberli, 2002: The new remote sensing-derived Swiss glacier inventory: I. Methods. *Annals of Glaciology*, 34: 355- 361.

Paul, F., A. Kääb, M. Maisch, T. Kellenberger, and W. Haeberli, 2004: Rapid disintegration of Alpine glaciers observed with satellite data, *Geophysical Research Letters,* 31, L21402, doi:10.1029/2004GL020816.

Post, A., D. Richardson, W.V. Tangborn, and F.L. Rosselot, 1971: Inventory of glaciers in the North Cascades, Washington. U.S. Geological Survey Professional Paper 705-A: 26pp.

Rahmstorf, S., 2007: A semi-empirical approach to projecting future sea-level rise. *Science*, 315, 5810: 368-370.

Raper, S.C.B. and R.J. Braithwaite, 2006: Low sea level rise projections from mountain glaciers and icecaps under global warming. *Nature*, 439, 19: 311-313.

Redmond K. T. and R. W. Koch, 1991: Surface climate and streamflow variability in the western United States and their relationship to large scale circulation indices. *Water Resources Research*, **27**: 2381-2399.

Ropelewski, C.F. and M.S. Halpert, 1986: North American precipitation and temperature patterns associated with the El Niño/Southern Oscillation (ENSO), *Monthy Weather Review*, 114, 12: 2352-2362.

Schuler, T., R. Hock, M. Jackson, H.Elvehøy, M. Braun, I. Brown, and J.O. Hagen, 2005: Distributed mass balance and climate sensitivity modelling of Engabreen, Norway. *Annals of Glaciology,* 42: 395-401.

Spicer, R.C., 1986: Glaciers in the Olympic Mountains, Washington: Present distribution and recent variations: Seattle, Wash. Unpublished Thesis (M.S.), University of Washington, 158pp.

Stahl, K., and R. D. Moore, 2006: Influence of watershed glacier coverage on summer streamflow in British Columbia, Canada. *Water Resources Research*, 42: W06201, doi:10.1029/2006WR005022.

Tangborn, W.V., 1999: A Mass Balance Model that Uses Low-altitude Meteorological Observations and the Area-Altitude Distribution of a Glacier. *Geografiska Annaler*, 81A, 4: 753-765.

Tangborn, W.V., A.G. Fountain, and W.G. Sikonia, 1990: Effect of area distribution with altitude on glacier mass balance – a comparison of North and South Klawati glaciers, Washington state, U.S.A., *Annals of Glaciology*, 14: 278-282.

Tangborn, W. and B. Rana, 2000: Mass balance and runoff of the partially debris covered Langtang Glacier, Nepal. In: *Debris-Covered Glaciers* [Nakawo, M., Raymond, C. F., and. Fountain, A. (eds.)]. International Association of Hydrological Sciences, Seattle, WA. IASH Publication, 264.

Walters, R.A. and M.F. Meier, 1989: Variability of glacier mass balances in western North America. In: *Aspects of Climate Variability in Pacific and Western Americas* [Peterson, D.H. (ed.)]. Geophysical Monograph, 55, American Geophysical Union, Washington, DC: pp.365-374.

Wolter, K., and M.S. Timlin, 1993: Monitoring ENSO in COADS with a seasonally adjusted principal component index. *Proceedings of the 17th Climate Diagnostics Workshop*, Norman, OK, NOAA/N MC/CAC, NSSL, Oklahoma Climate Survey, CIMMS and the School of Meteorology, University of Oklahoma: 52-57.

Wood, J.A., 2006: Using the Precipitation Temperature Area Altitude model to simulate glacier mass balance in the North Cascades. Unpublished Thesis (M.S.), Western Washington University.

Zhang, J, U.S. Bhatt, W.V. Tangborn, and C.S. Lingle, 2007: Climate downscaling for estimating glacier mass balances in northwestern North America: Validation with a USGS benchmark glacier. *Geophysical Research Letters*, 34: L21505, doi:10.1029/2007GL031139.